# CHAPTER V

# CONCLUSION

This thesis is concerned with the response of dynamic interaction between an axisymmetric loaded circular plate and two different types of poroelastic medium, i.e., a homogeneous poroelastic half-space and a multi-layered poroelastic half-space. The interface between the circular plate and the half-space is assumed to be smooth. The plate, which is either fully permeable and impermeable, subjected to axisymmetric time-harmonic vertical loading. The cases of a plate on the surface and deeply buried in a poroelastic medium are the two limiting cases of the generalized problem under consideration in the present study. The elastodynamic principle and the discretization technique are employed to study this dynamic interaction problem. The influence functions for homogeneous poroelastic half-space are directly obtained from solutions given explicitly in section 3.1 together with arbitrary functions given in Appendix B. The exact stiffness matrix scheme is used to determine the influence functions for multi-layered poroelastic half-space.

The convergence and numerical stability of the present solution scheme with respect to $N$ and $Ne$ are first studied. From this convergence study, the numerical solutions are found to be stable when $N$=8 and $Ne$=20. In addition, the accuracy of the present scheme is confirmed by comparing with the existing studies.

Numerical results presented in Chapter IV indicate that the interaction problem is governed by a complicated combination of several parameters. The influences from those parameters on the plate response are summarized below.

1. Vertical displacements of a plate are significantly influenced by the depth of embedment and the frequency of excitation. The central displacement of a buried plate is smaller than that of the surface plate but shows more oscillations with frequency.

2. The poroelastic material properties and the hydraulic boundary conditions of the plate have a significant influence on vertical vibrations of the plate when the non-dimensional frequency $\delta > 2$.

3. For the effect of the plate flexibility, the displacements increase with increasing the relative flexibility $\gamma$. This effect is negligible when $\gamma \geq 1000$.

4. The plate displacements are significantly influenced by the layer thickness when $\delta < 2.5$.

5. For the load transfer mechanism, the applied load is mainly carried through the solid skeleton for a low frequency. For a high frequency, the load transfer takes place through both solid and fluid phases of a soil medium.

The solutions presented in this study are useful in studying the response of buried foundations and anchors in poroelastic soils. In addition, the Green 's functions of both homogeneous poroelastic half-space and multi-layered poroelastic half-space can be used in Boundary Element analysis to study other geomechanics problems involving poroelastic media such as vibrations in piles and pile groups as well as scattering of seismic waves by cavities or inclusions in multi-layered poroelastic soils.

Table 1. Convergence of influence functions of a homogeneous poroelastic half-space with respect to $\xi_L$

| | $\mu u_{zz}(0,a)/f_o a$ | | $\mu u_{zp}(0,a)/f_o a$ | | $\mu w_{zz}(0,a)/f_o a$ | |
|---|---|---|---|---|---|---|
| $\xi_L$ | Re | Im | Re | Im | Re | Im |
| 20 | 0.2565 | -0.3201 | 0.1278 | -0.3115 | -0.1210 | -0.00097 |
| 40 | 0.2593 | -0.3201 | 0.1296 | -0.3118 | -0.1219 | -0.00135 |
| 60 | 0.2598 | -0.3201 | 0.1300 | -0.3119 | -0.1221 | -0.00144 |
| 80 | 0.2596 | -0.3201 | 0.1299 | -0.3119 | -0.1220 | -0.00136 |
| 100 | 0.2592 | -0.3201 | 0.1296 | -0.3118 | -0.1218 | -0.00135 |
| 120 | 0.2592 | -0.3201 | 0.1296 | -0.3118 | -0.1218 | -0.00135 |

Table 2. Convergence of solution with $N$ and $Ne$ for an elastic circular plate resting on a homogeneous poroelastic half-space

| | $\mathrm{Re}\left[w_p(0)\mu/(\delta f_o)\right]$ | | | | $\mathrm{Im}\left[w_p(0)\mu/(\delta f_o)\right]$ | | | |
|---|---|---|---|---|---|---|---|---|
| $N$ | $Ne=10$ | $Ne=15$ | $Ne=20$ | $Ne=25$ | $Ne=10$ | $Ne=15$ | $Ne=20$ | $Ne=25$ |
| 2 | 0.585 | 0.580 | 0.575 | 0.572 | -0.523 | -0.521 | -0.519 | -0.518 |
| 4 | 0.896 | 0.896 | 0.896 | 0.896 | -0.642 | -0.642 | -0.642 | -0.642 |
| 6 | 0.899 | 0.900 | 0.901 | 0.901 | -0.643 | -0.643 | -0.643 | -0.642 |
| 8 | 0.899 | 0.900 | 0.901 | 0.901 | -0.643 | -0.643 | -0.643 | -0.643 |

Table 3. Material properties of a homogeneous poroelastic half-space

| | $\mu^{\dagger}$ | $\lambda^{\dagger}$ | $M^{\dagger}$ | $\rho^{\ddagger}$ | $\rho_f{}^{\ddagger}$ | $m^{\ddagger}$ | $\alpha$ | $b^{\#}$ |
|---|---|---|---|---|---|---|---|---|
| Material HA | 2.0 | 2.0 | 24.4 | 2.0 | 1.06 | 2.2 | 0.97 | $6.32 \times 10^{2}$ |
| Material HA | 2.0 | 2.0 | 24.4 | 2.0 | 1.06 | 2.2 | 0.97 | $1.45 \times 10^{6}$ |
| Material HA | 2.0 | 2.0 | 24.4 | 2.0 | 1.06 | 2.2 | 0.97 | $6.32 \times 10^{6}$ |
| Material HA | 2.0 | 2.0 | 24.4 | 2.0 | 1.06 | 2.2 | 0.97 | $6.32 \times 10^{7}$ |
| Material HA | 2.0 | 2.0 | 0.0 | 2.0 | 0.0 | 0.0 | 0.0 | 0.0 |

$^{\dagger}$ x $10^{8}$ N/m$^{2}$ $^{\ddagger}$ x $10^{3}$ kg/m$^{3}$ $^{\#}$ N s/m$^{4}$

Table 4. Material properties of a three-layered poroelastic half-space

| | $\mu^{\dagger}$ | $\lambda^{\dagger}$ | $M^{\dagger}$ | $\rho^{\ddagger}$ | $\rho_f{}^{\ddagger}$ | $m^{\ddagger}$ | $\alpha$ |
|---|---|---|---|---|---|---|---|
| First layer | 2.5 | 5.0 | 25.0 | 2.0 | 1.0 | 3.0 | 0.95 |
| Second layer | 1.25 | 1.88 | 18.8 | 1.6 | 1.0 | 1.8 | 0.98 |
| Half space | 10.0 | 10.0 | 20.0 | 2.4 | 1.0 | 4.8 | 0.9 |

$^{\dagger}$ x $10^{8}$ N/m$^{2}$ $^{\ddagger}$ x $10^{3}$ kg/m$^{3}$

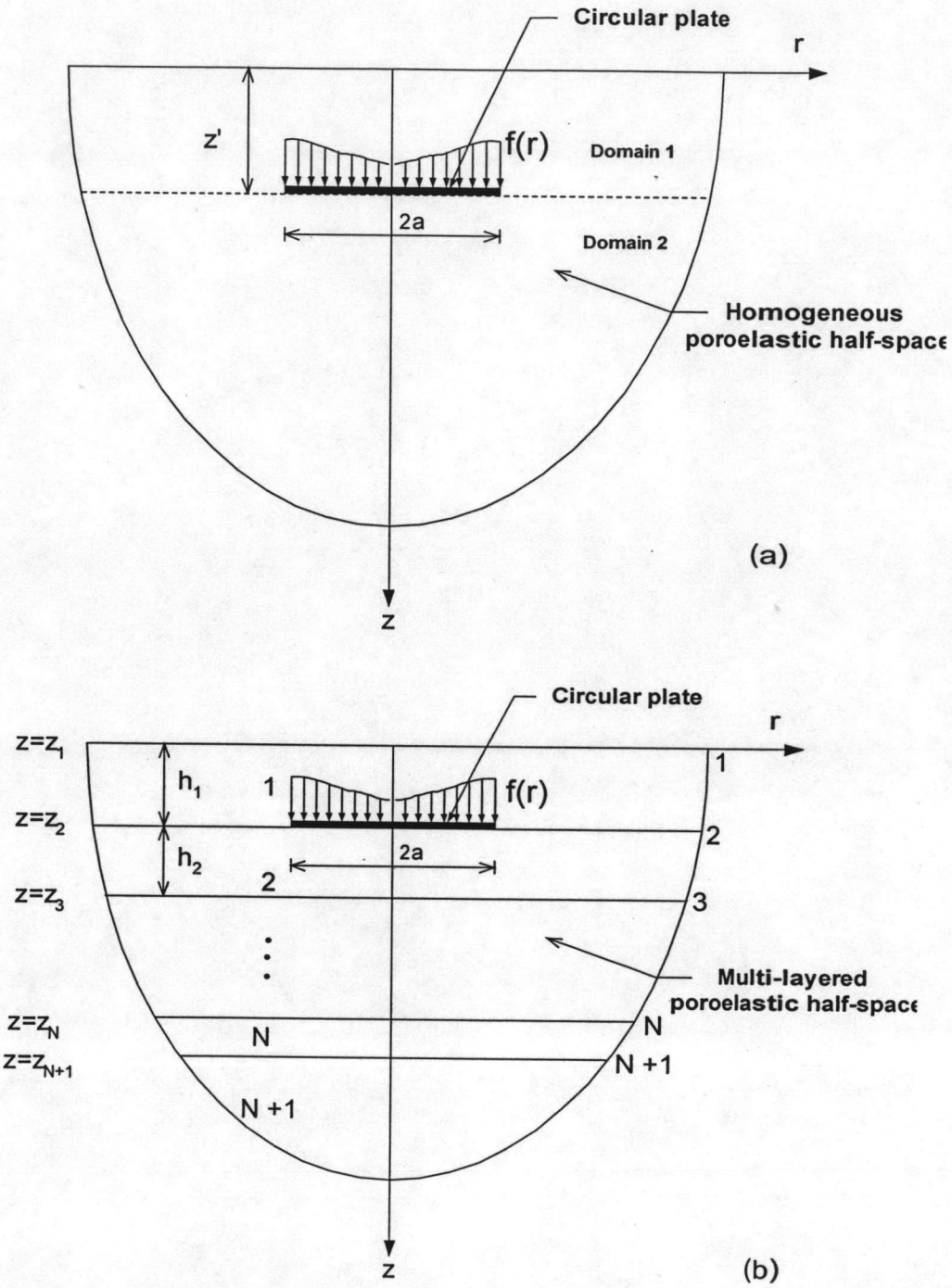


Figure 1. Geometry of the circular plate-poroelastic half-space system considered in this study

(a) Circular plate-Homogeneous poroelastic half-space

(b) Circular plate-Multi-layered poroelastic half-space.

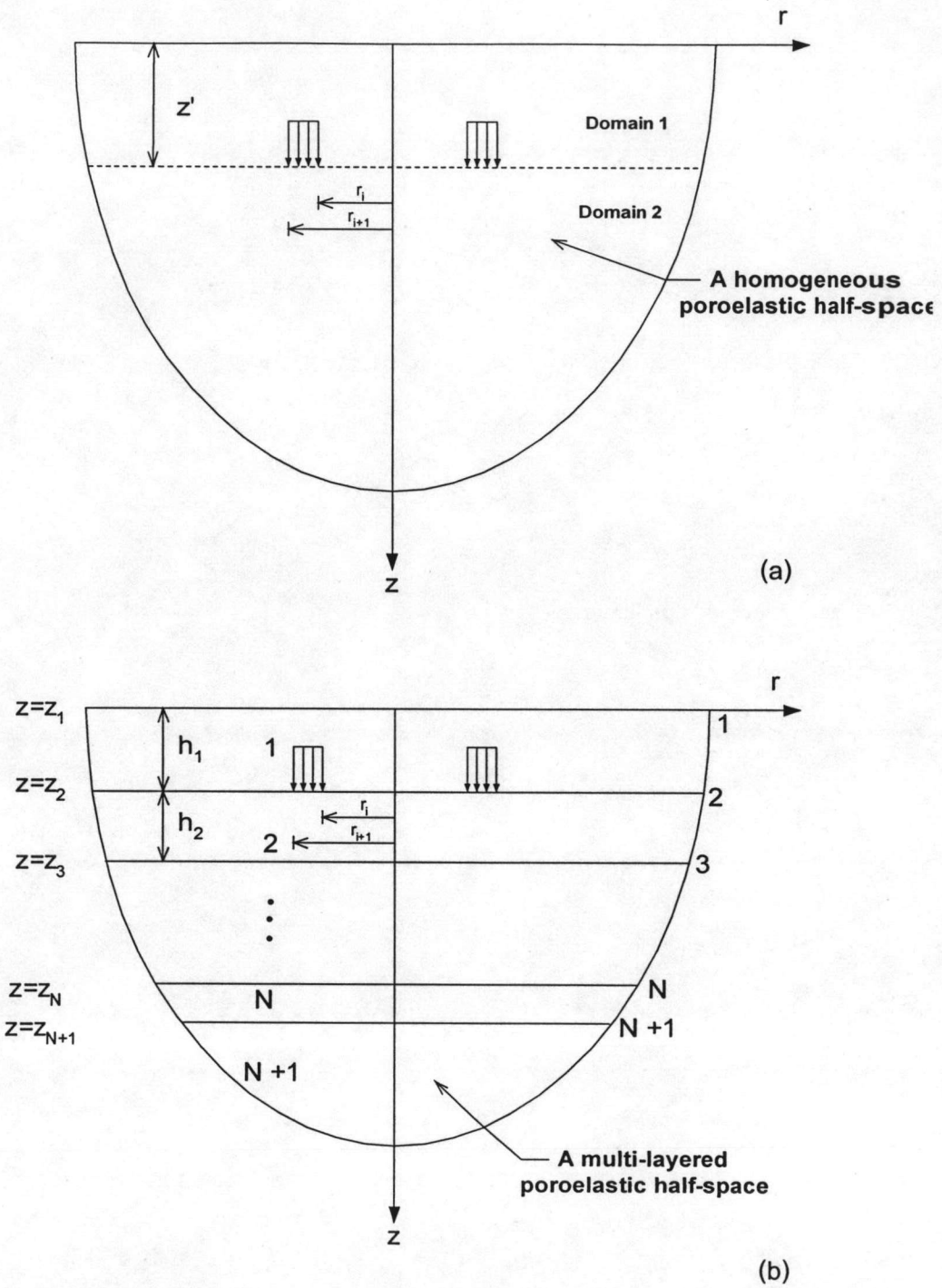


Figure 2. Unit vertical pressure acting over an annular region in (a) Homogeneous poroelastic half-space (b) Multi-layered poroelastic half-space

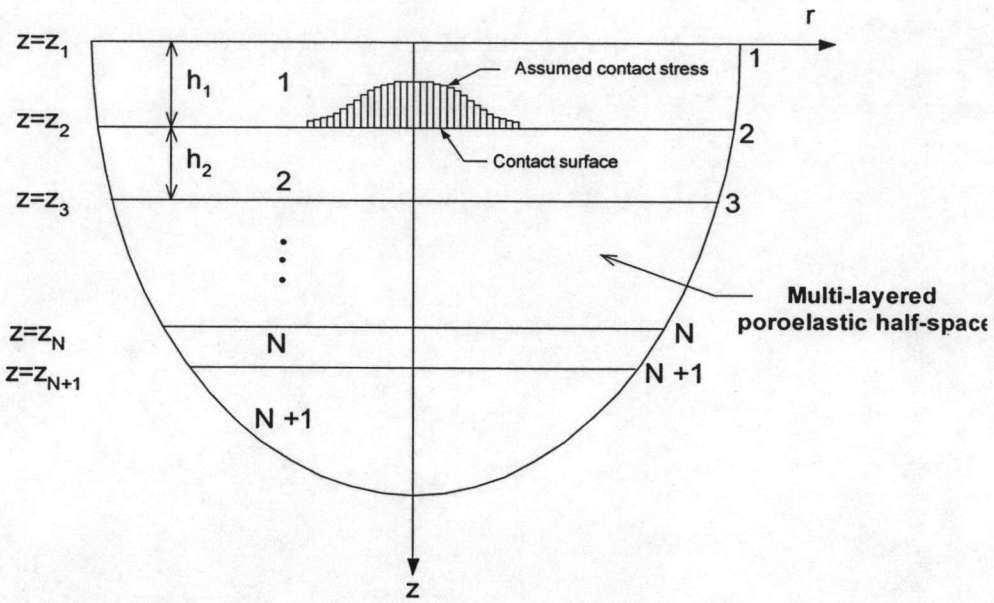


Figure 3. Assumed uniform contact stress over discretized circular area

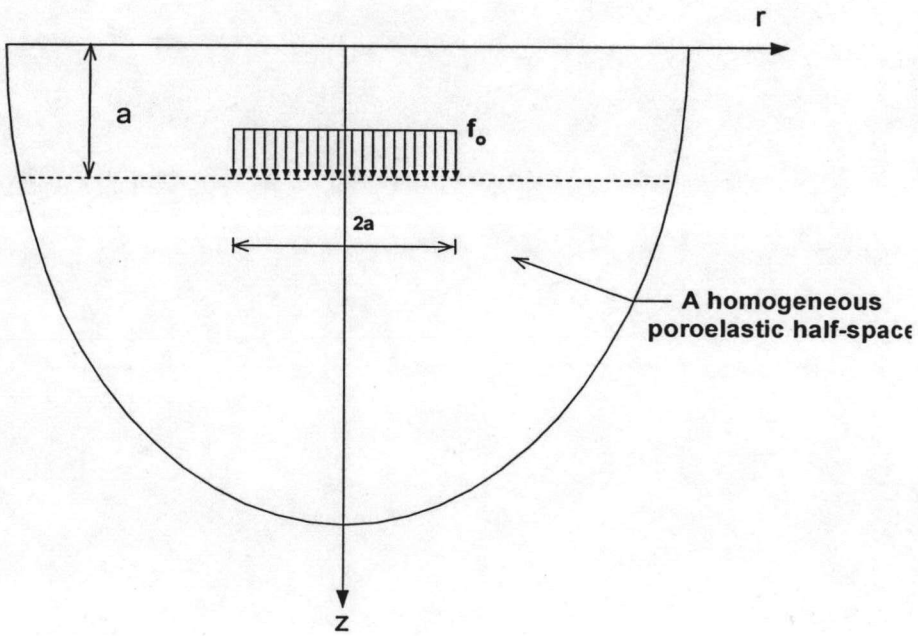


Figure 4. A homogeneous poroelastic half-space subjected to uniformly distributed loading

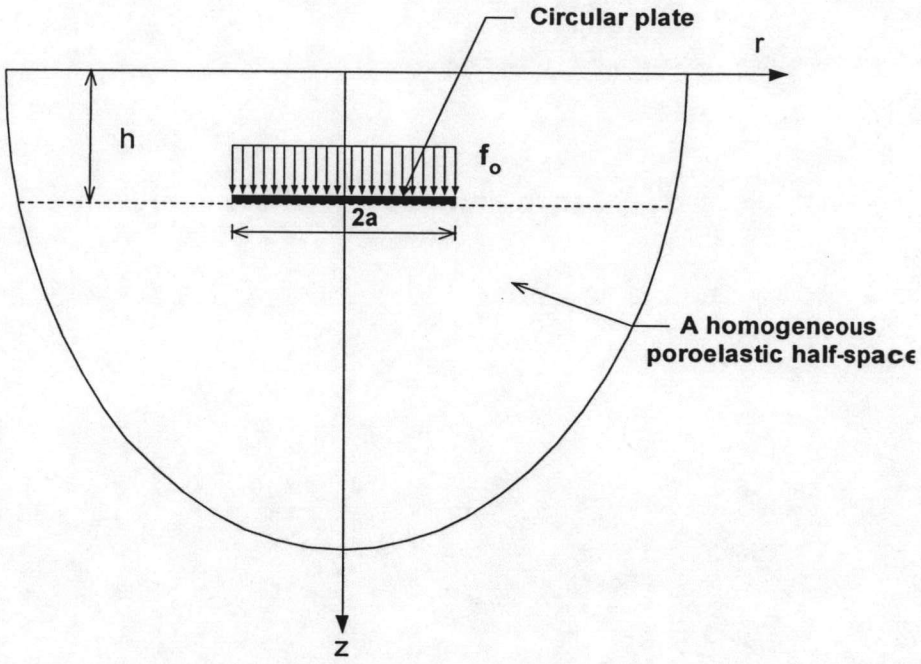


Figure 5. Elastic circular plate in a homogeneous poroelastic half-space considered in the numerical study

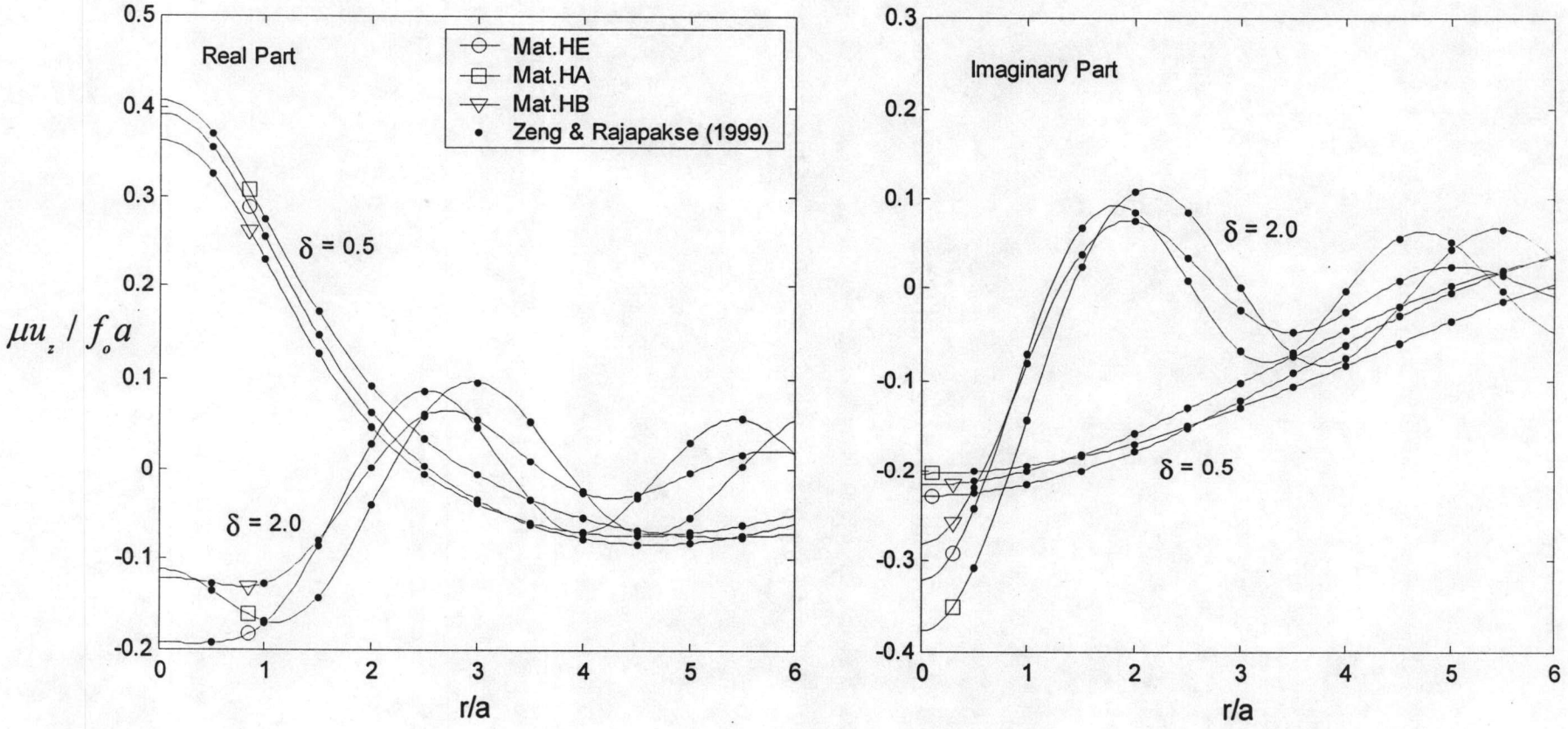


Figure 6. Comparison of vertical displacements along the free surface due to buried uniform vertical patch load at $z' = a$ in a homogeneous poroelastic half-space

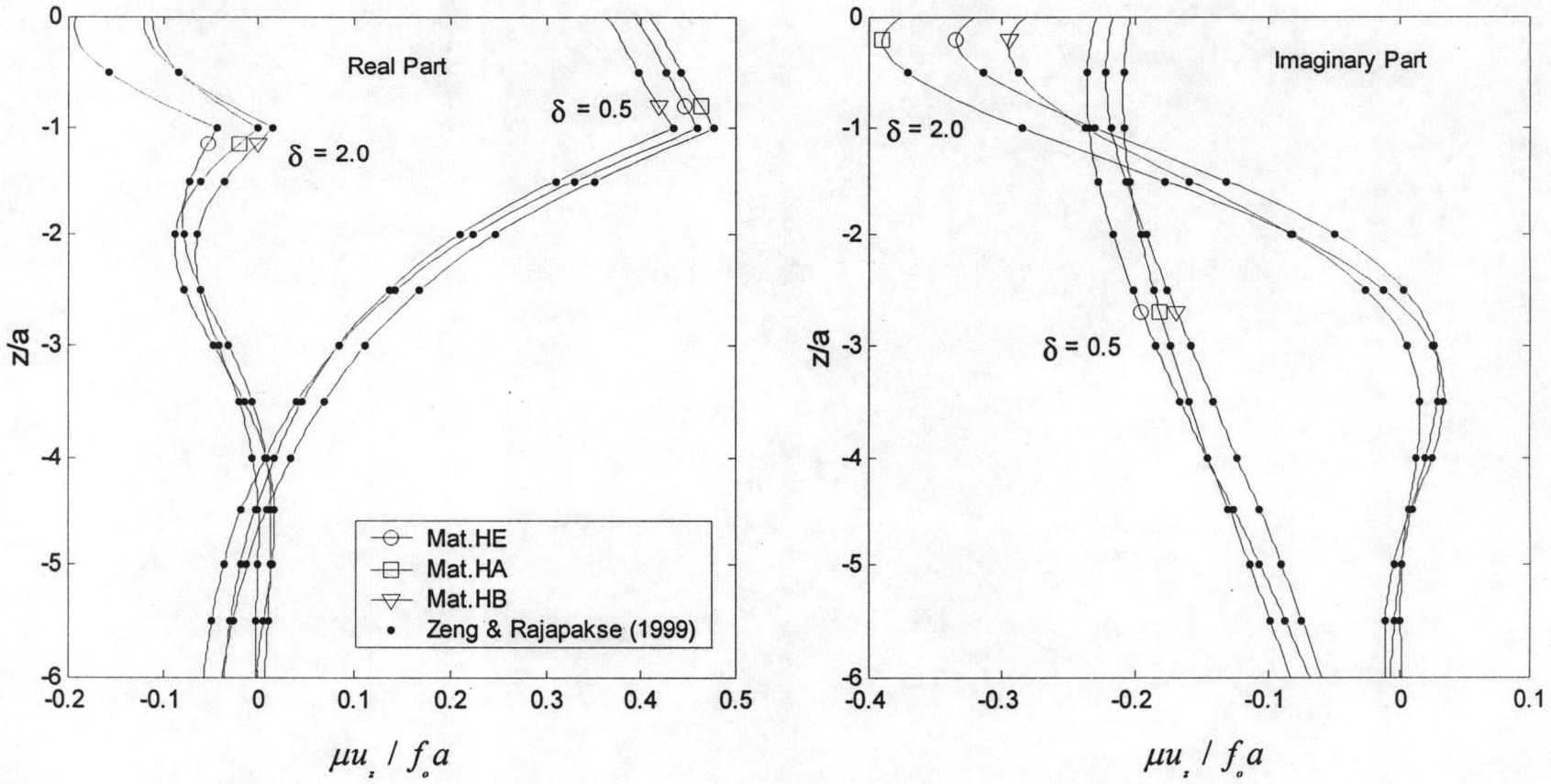


Figure 7. Comparison of vertical displacements along the $z$-axis due to buried uniform vertical patch load at $z' = a$ in a homogeneous poroelastic half-space

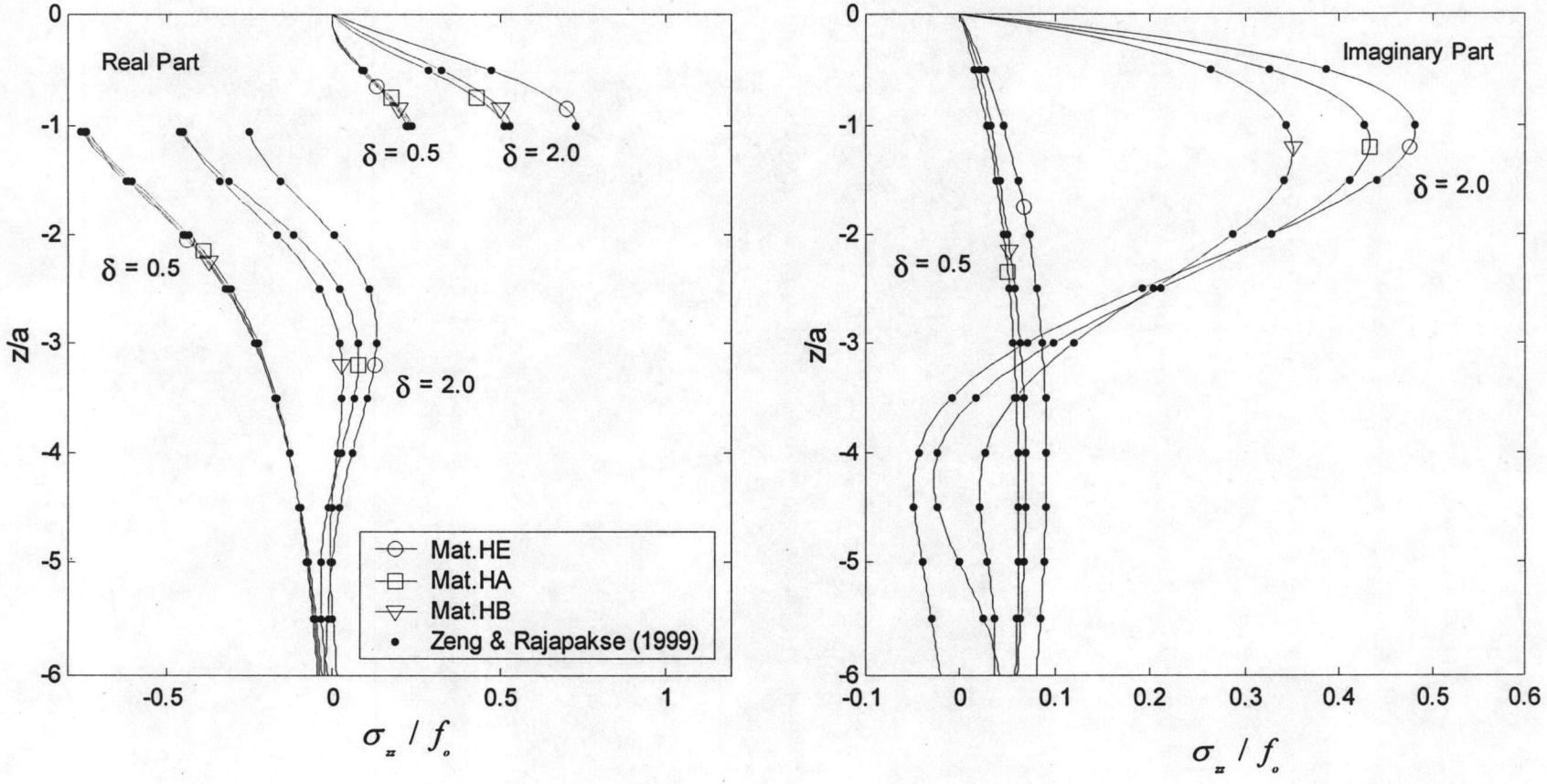


Figure 8. Comparison of vertical stresses along the $z$ -axis due to buried uniform vertical patch load at $z' = a$ in a homogeneous poroelastic half-space

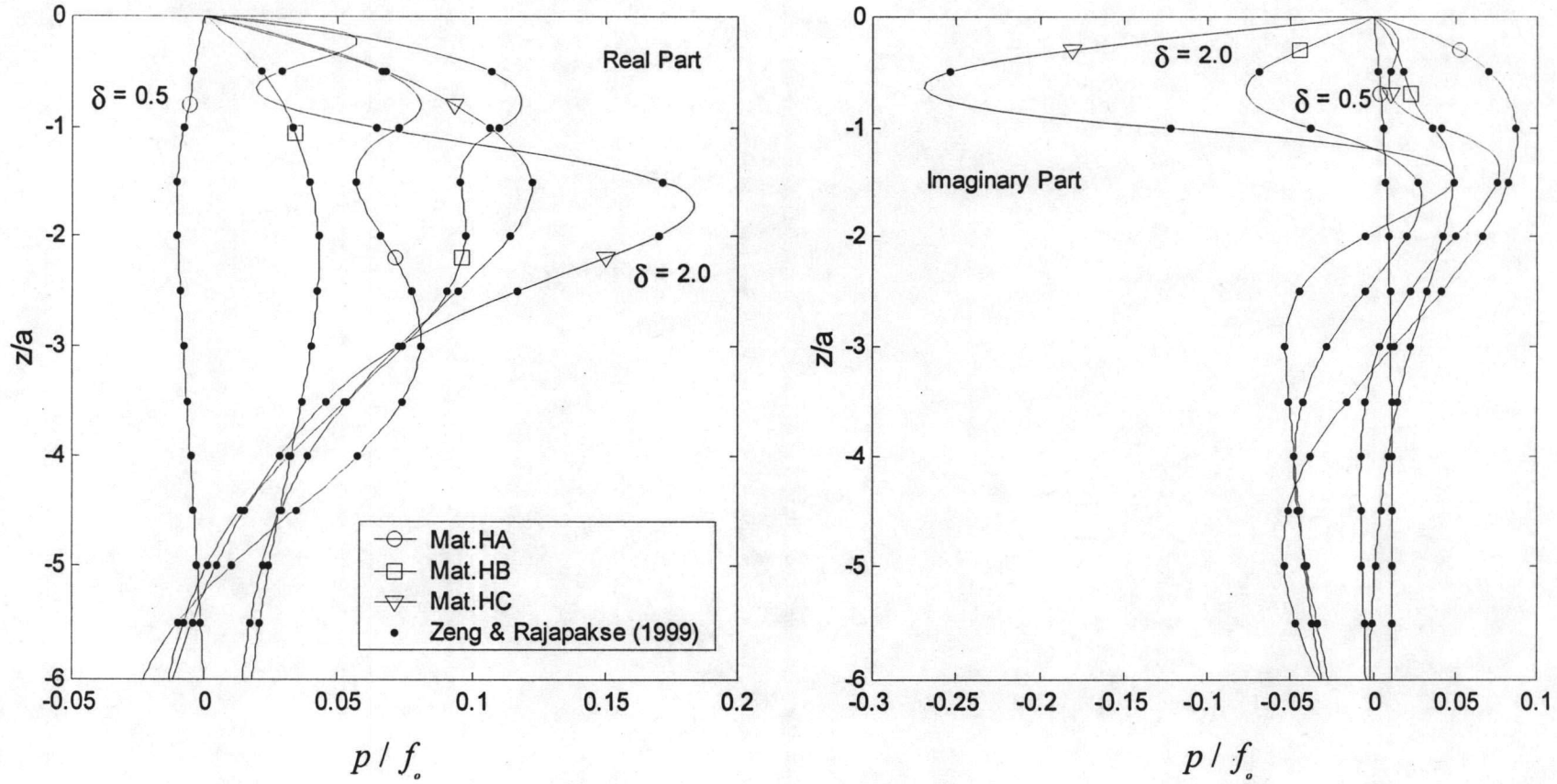


Figure 9. Comparison of pore pressure along the $z$-axis due to buried uniform vertical patch load at $z' = a$ in a homogeneous poroelastic half-space

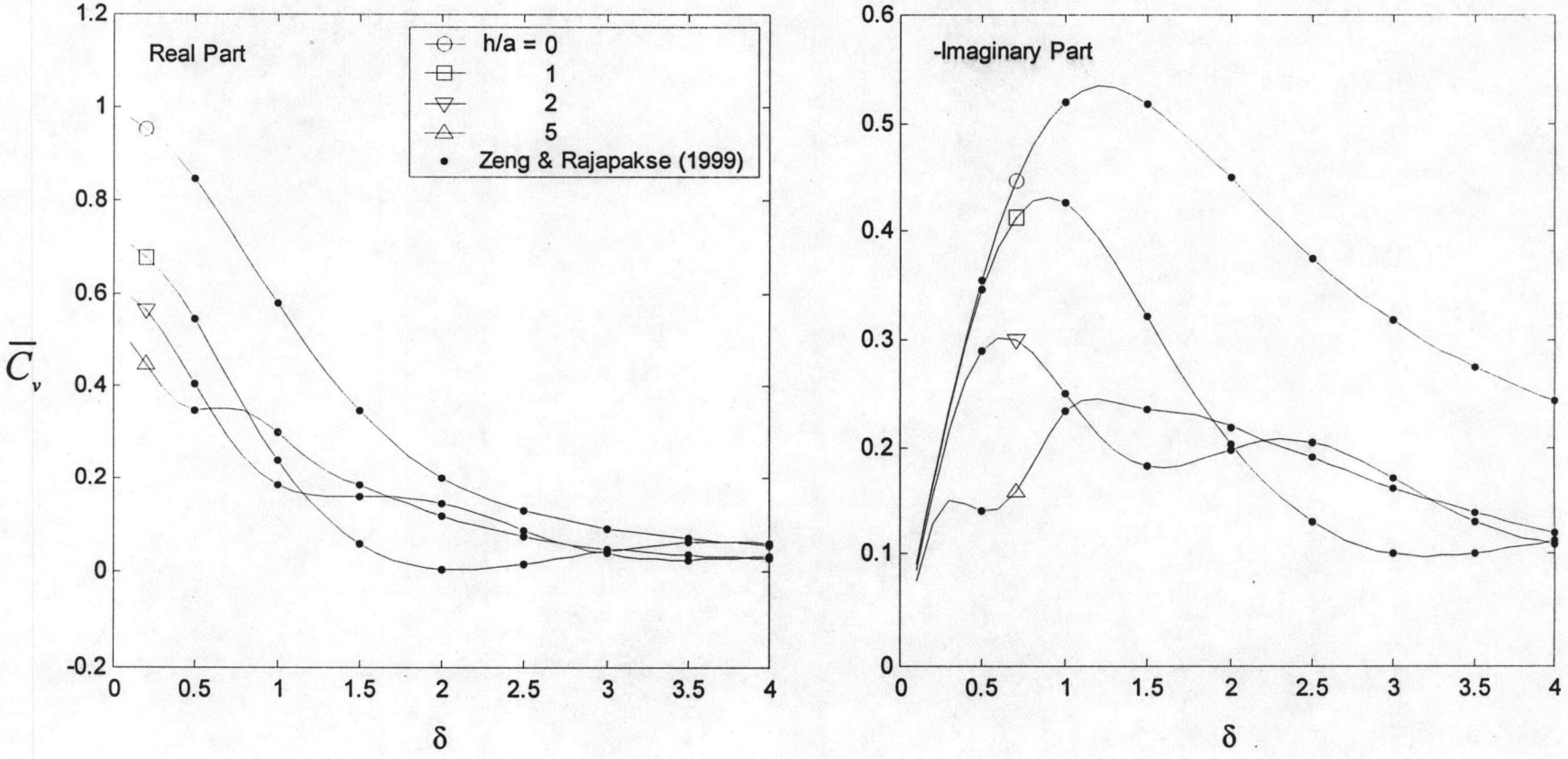


Figure 10. Comparison of vertical compliances of a permeable rigid circular plate in a homogeneous poroelastic half-space with different depths of embedment

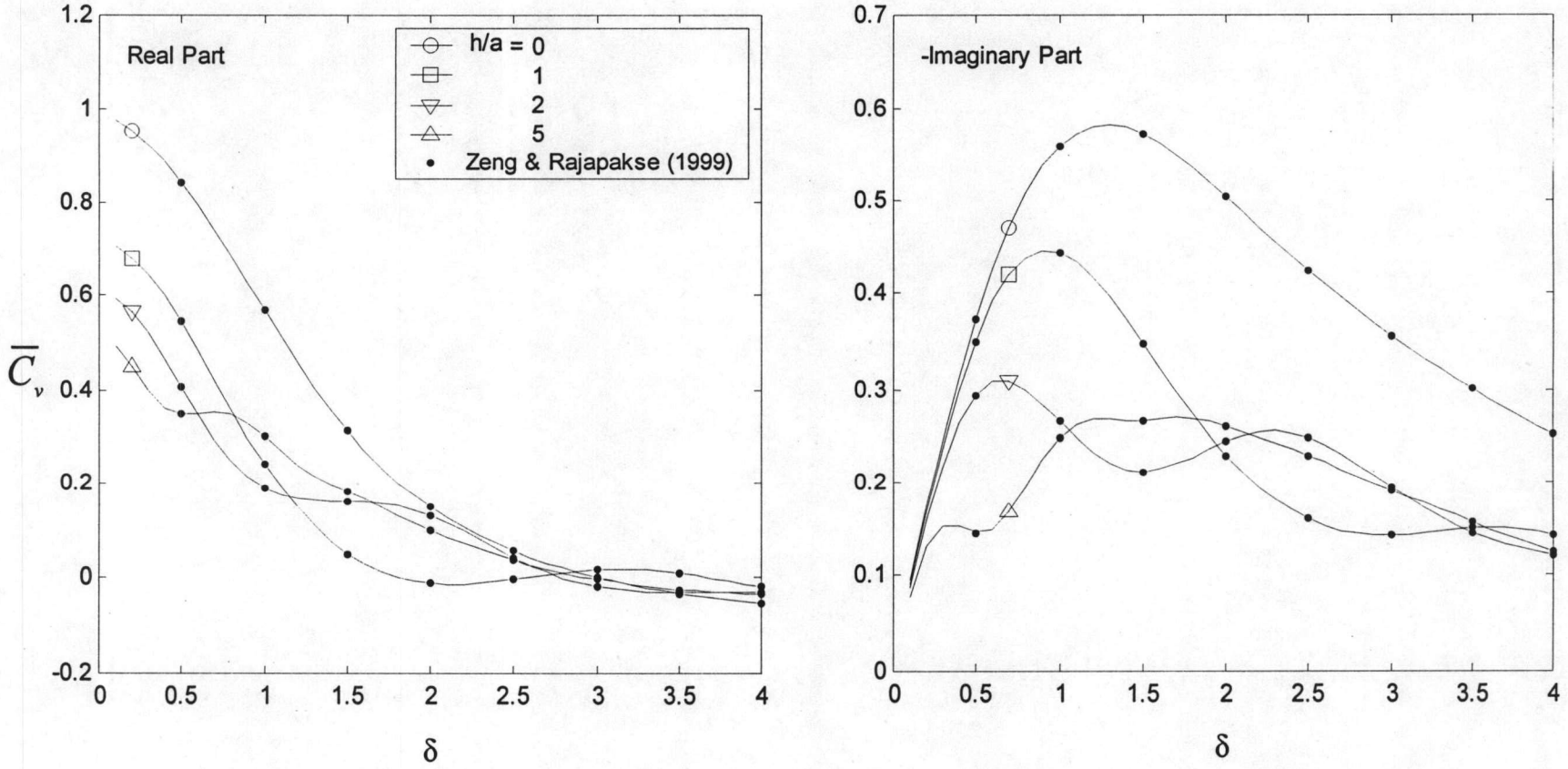


Figure 11. Comparison of vertical compliances of an impermeable rigid circular plate in a homogeneous poroelastic half-space with different depths of embedment

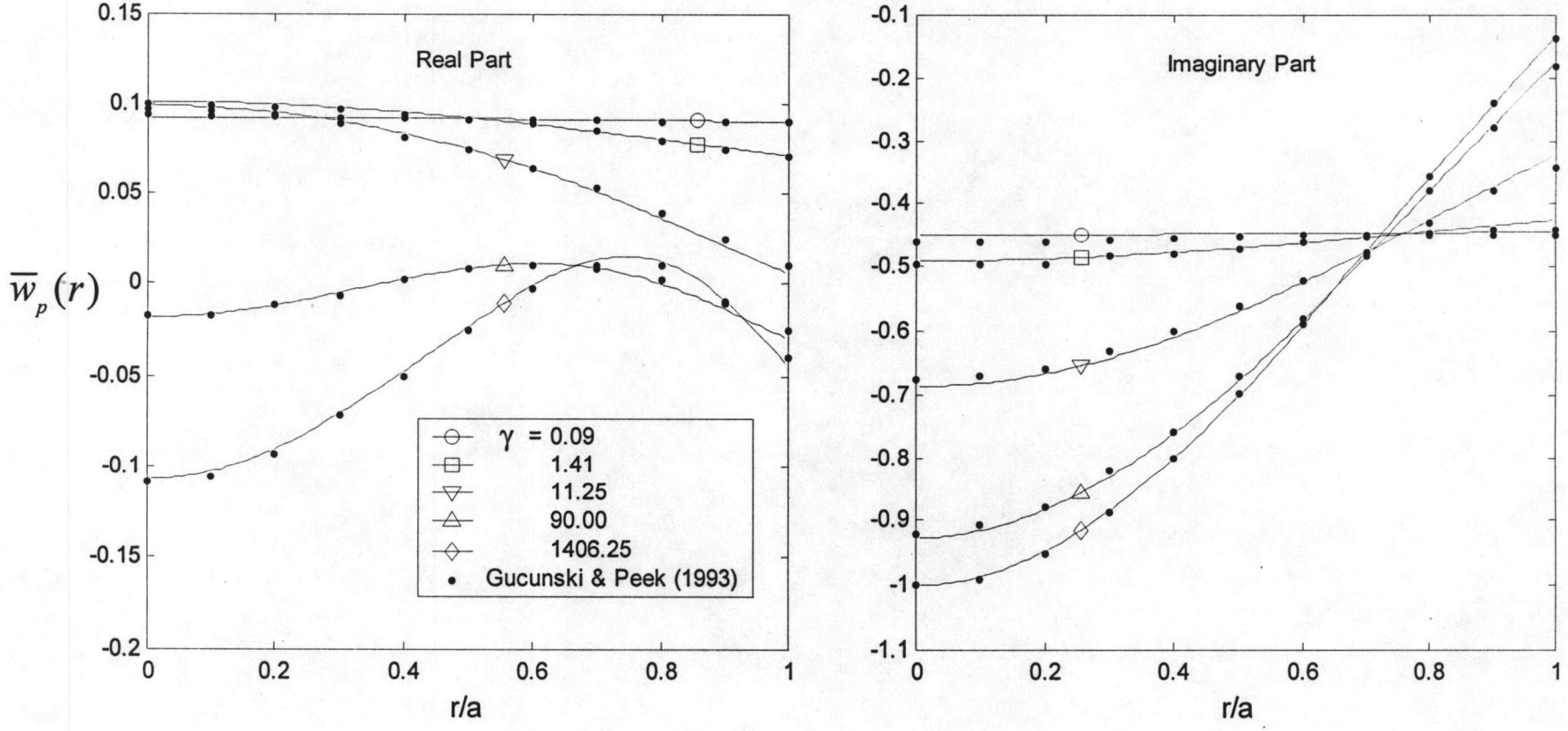


Figure 12. Comparison of displacement profiles of a circular plate resting on a homogeneous elastic half-space with different relative flexibilities

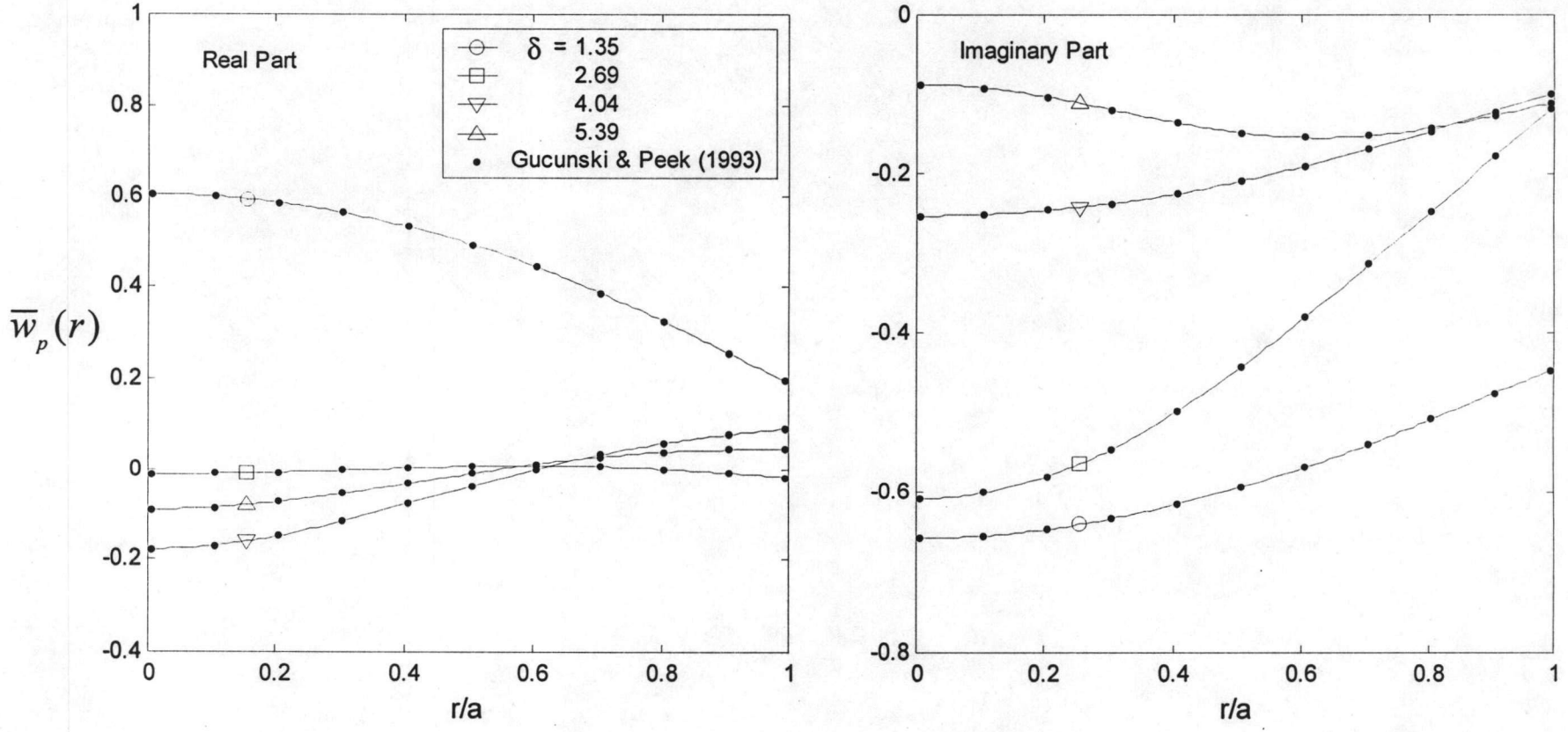


Figure 13. Comparison of displacement profiles of a circular plate resting on a homogeneous elastic half-space with different frequencies

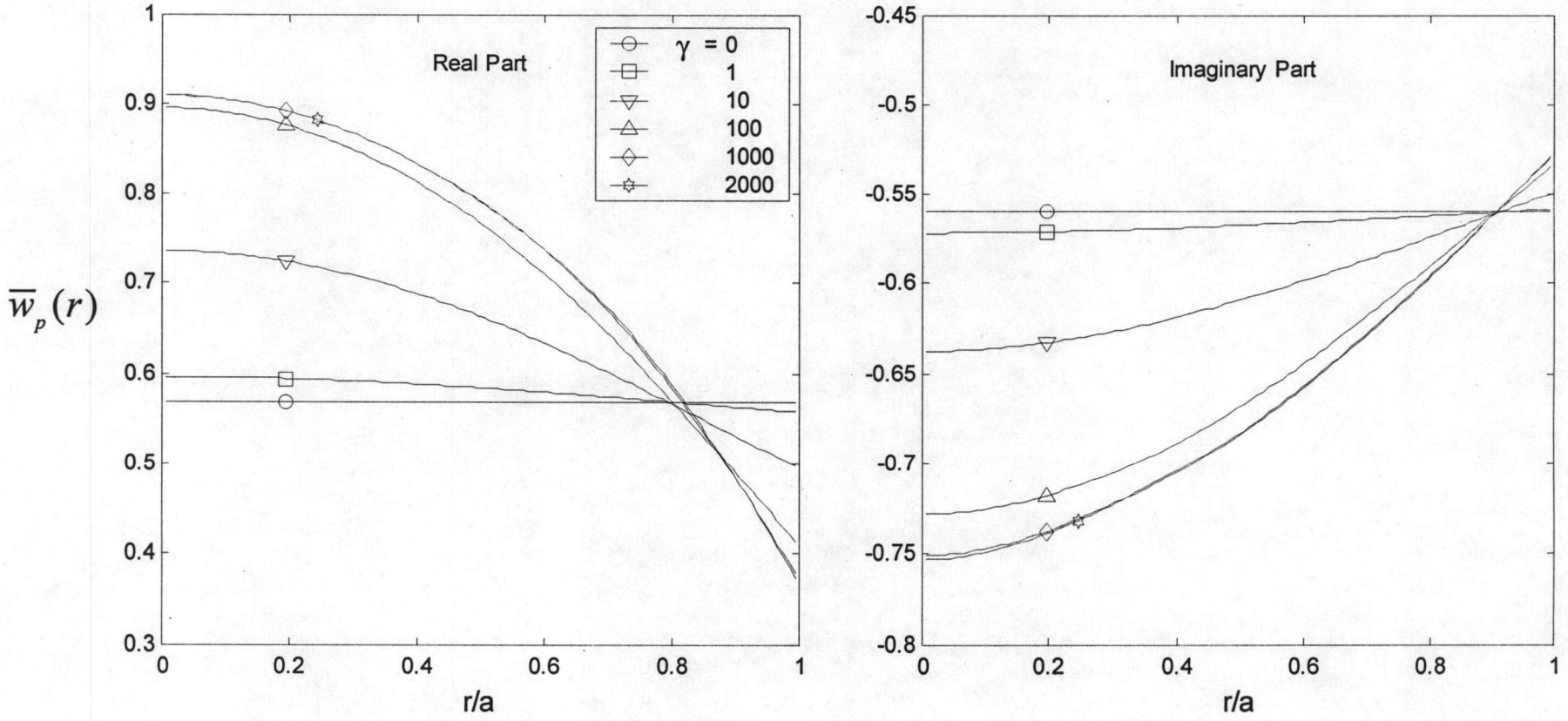


Figure 14. Displacement profiles of an impermeable circular plate resting on a homogeneous poroelastic half-space for different relative flexibilities ($\delta$ =1)

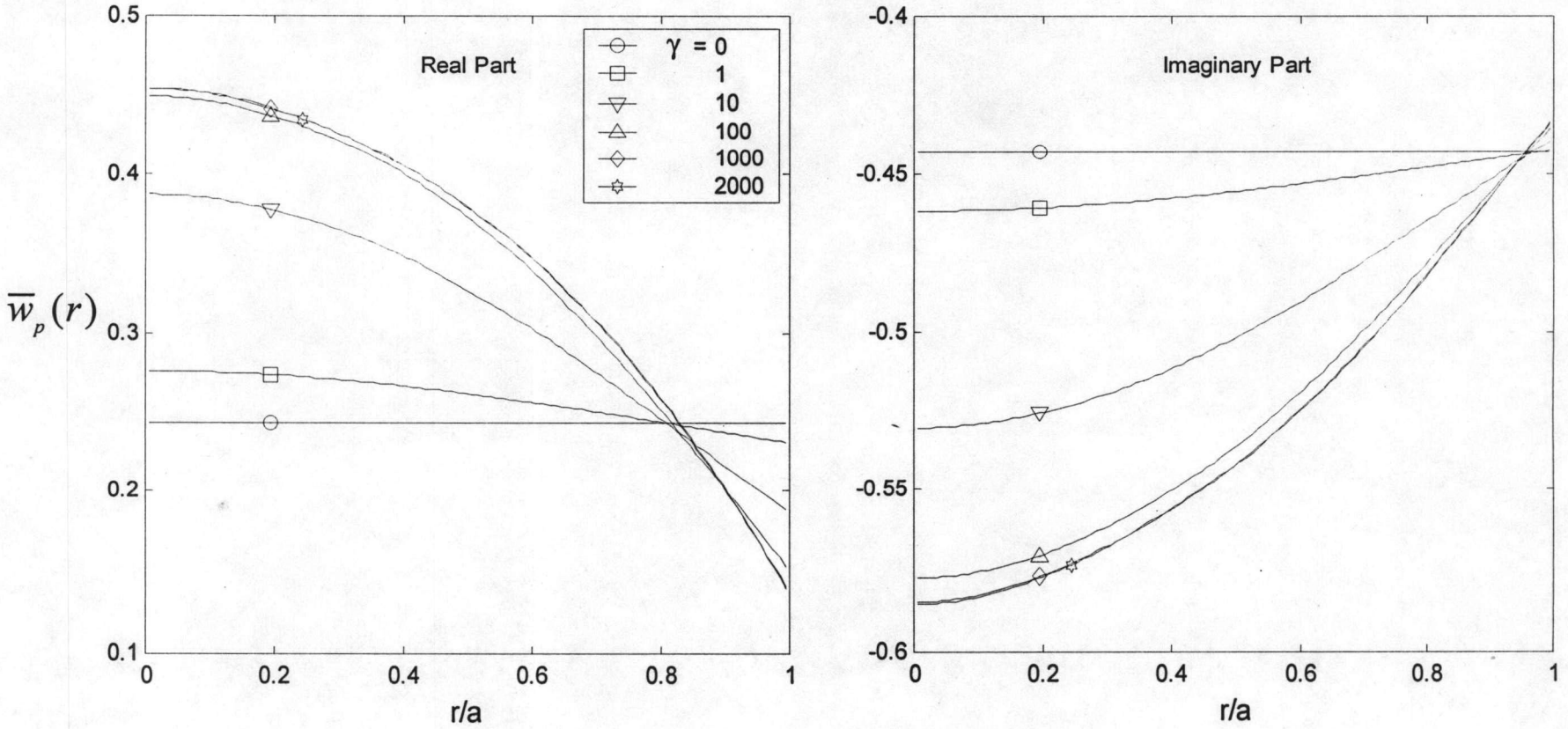


Figure 15. Displacement profiles of an impermeable circular plate buried in ($h/a=1$) a homogeneous poroelastic half-space for different relative flexibilities ($\delta$ =1)

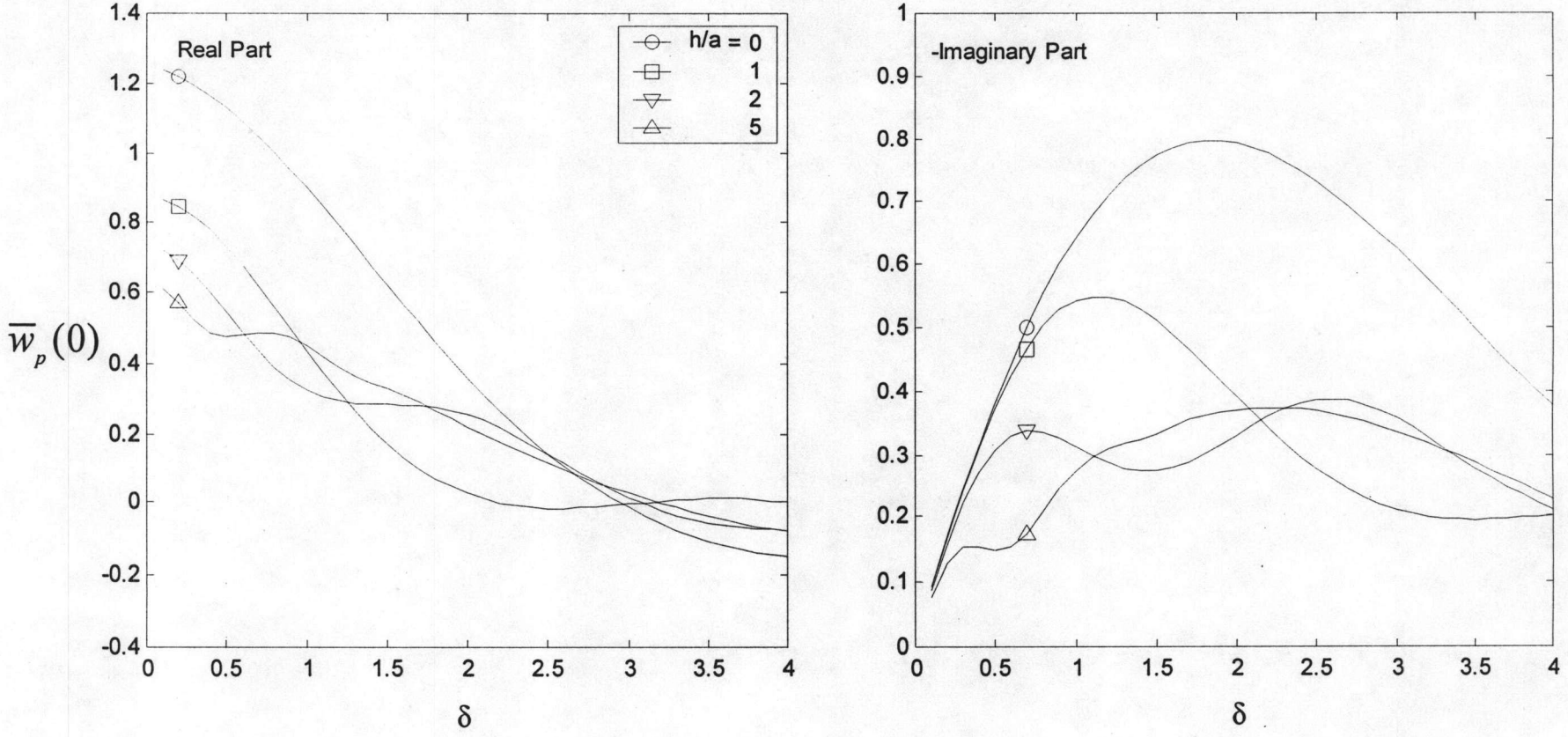


Figure 16. Central displacement of a permeable circular plate in a homogeneous poroelastic half-space with different depths of embedment

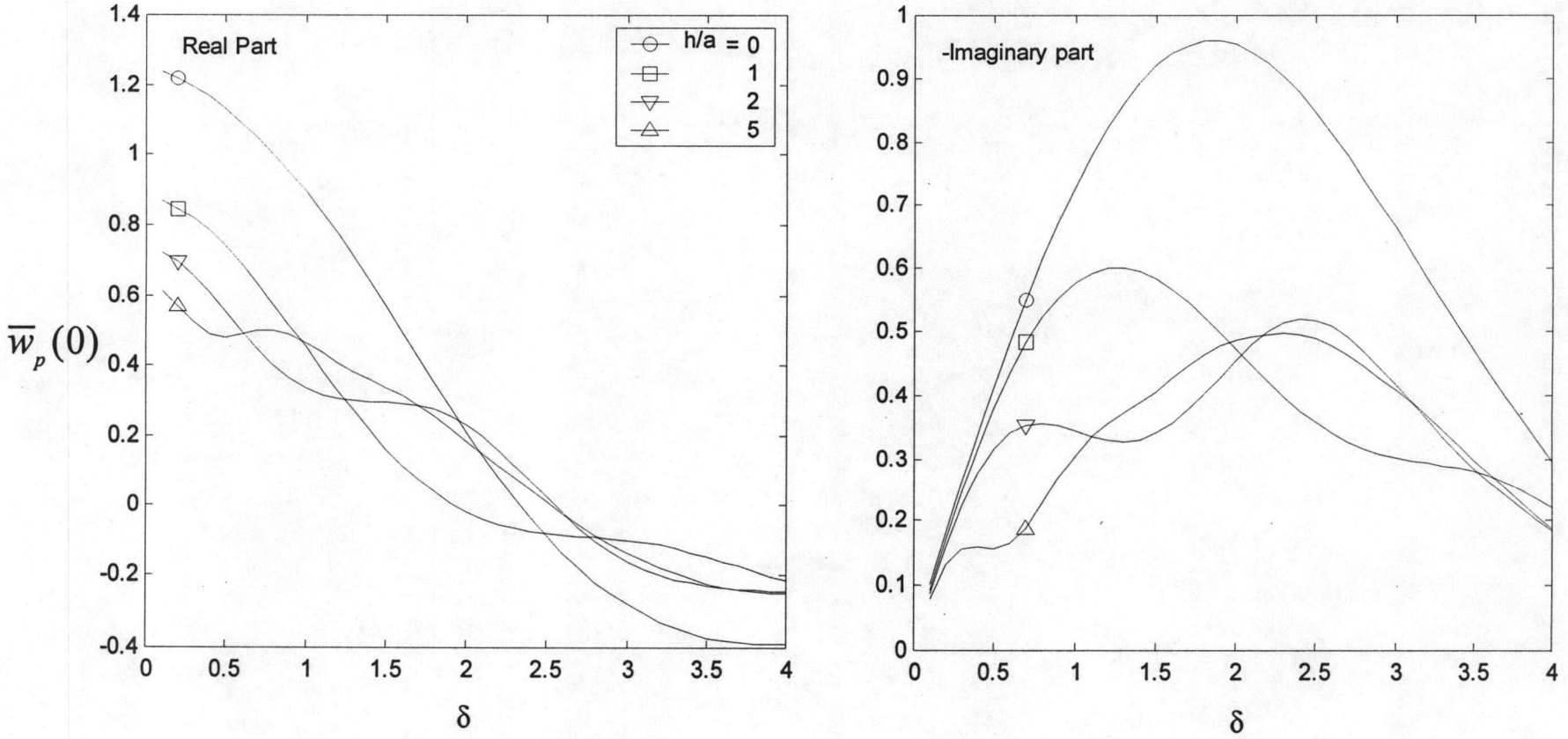


Figure 17. Central displacement of an impermeable circular plate in a homogeneous poroelastic half-space with different depths of embedment

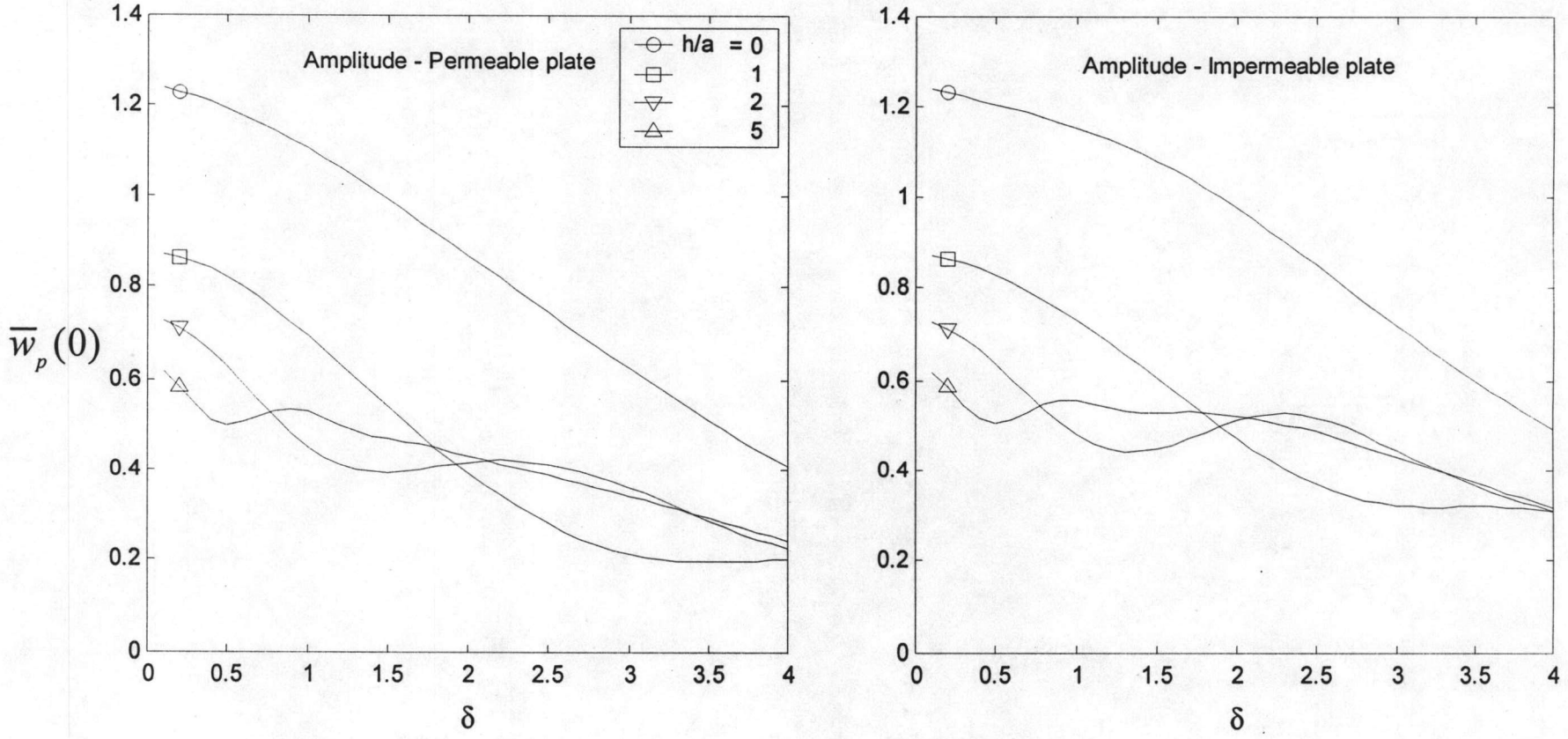


Figure 18. Amplitude of central displacement of a circular plate in a homogeneous poroelastic half-space with different depths of embedment

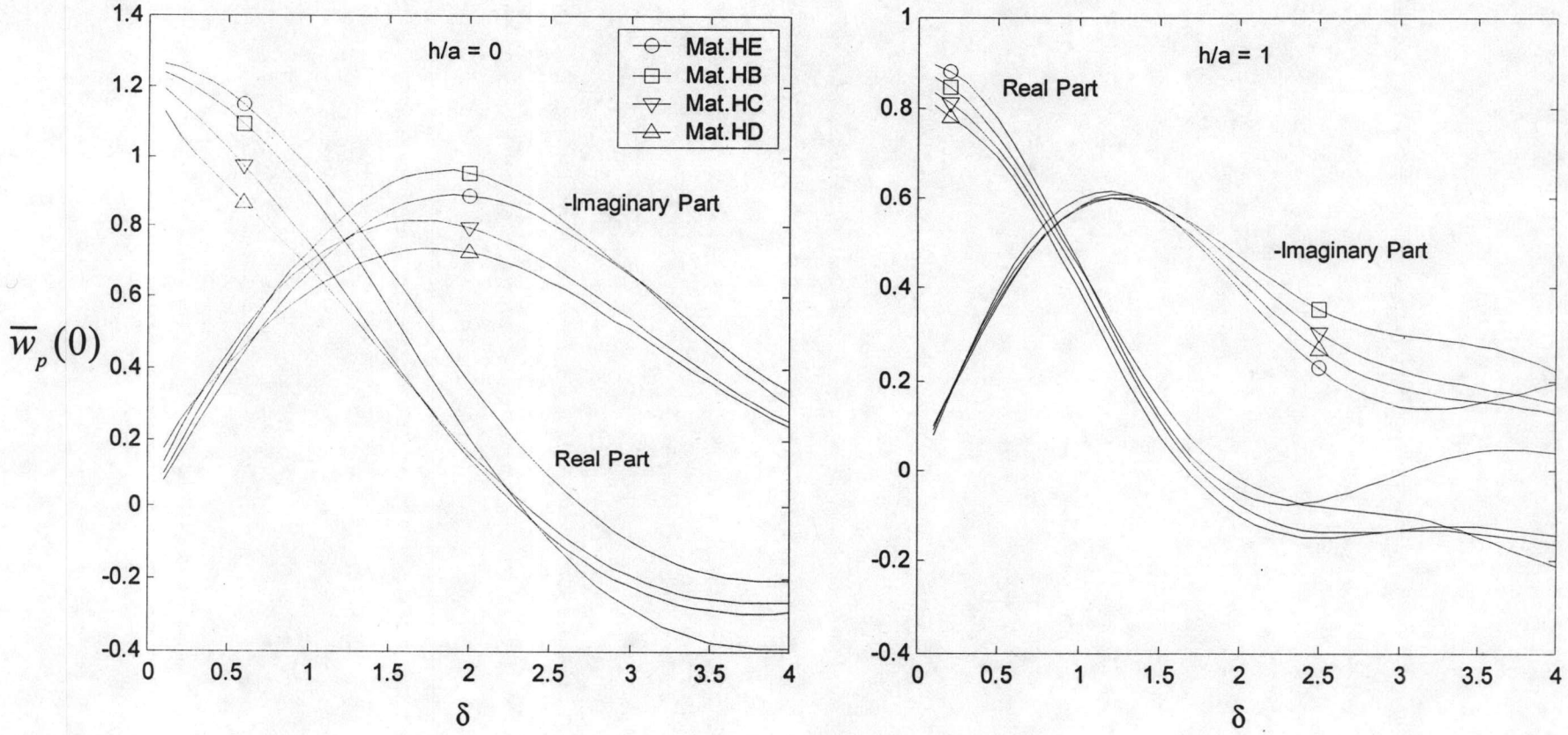


Figure 19. Central displacement of an impermeable circular plate in a different poroelastic media

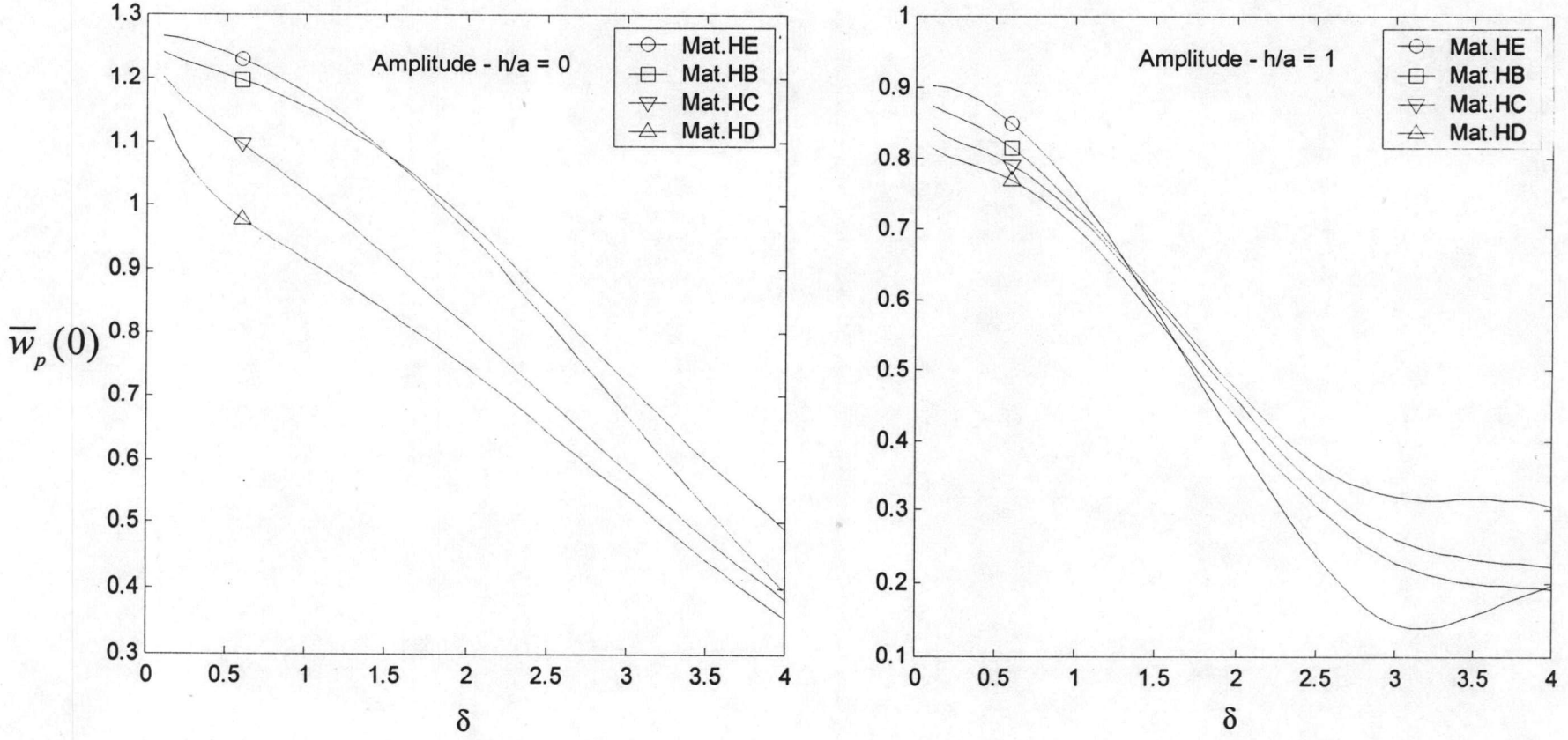


Figure 20. Amplitude of central displacement of an impermeable circular plate in a different poroelastic media

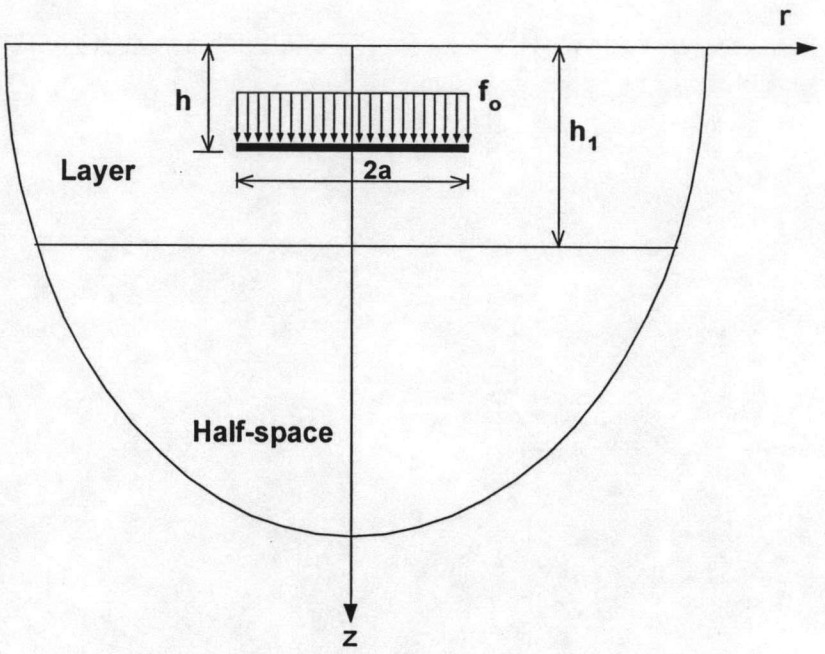


(a) Two-layered system

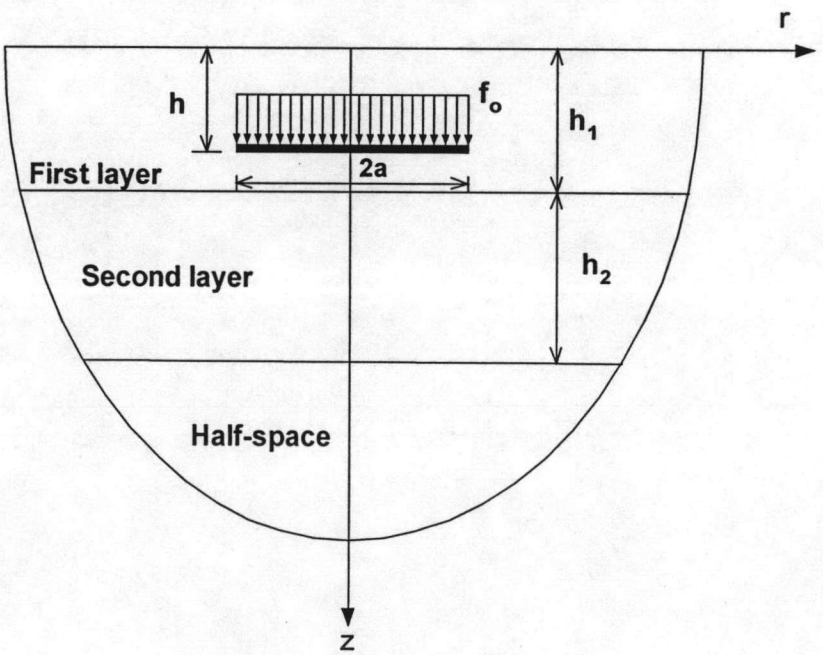


(b) Three-layered system

Figure 21. Elastic circular plate in a multi-layered poroelastic half-space considered in numerical study

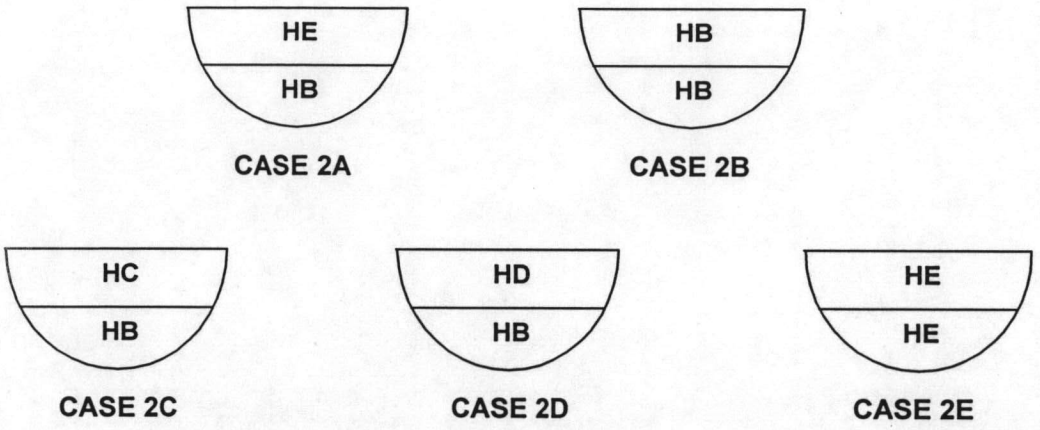


Figure 22. Fives cases considered in two-layered system

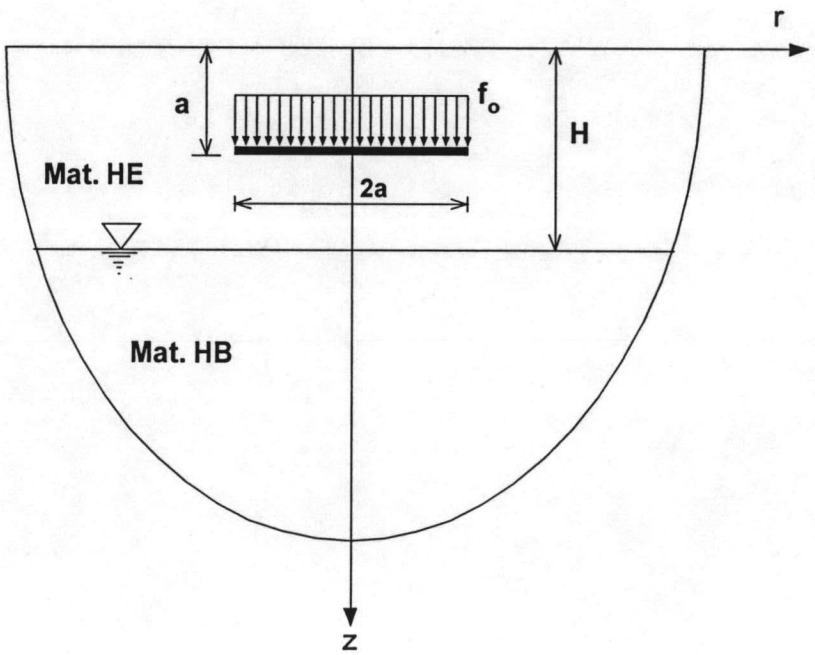


Figure 23. Circular plate in a partially saturated half-space

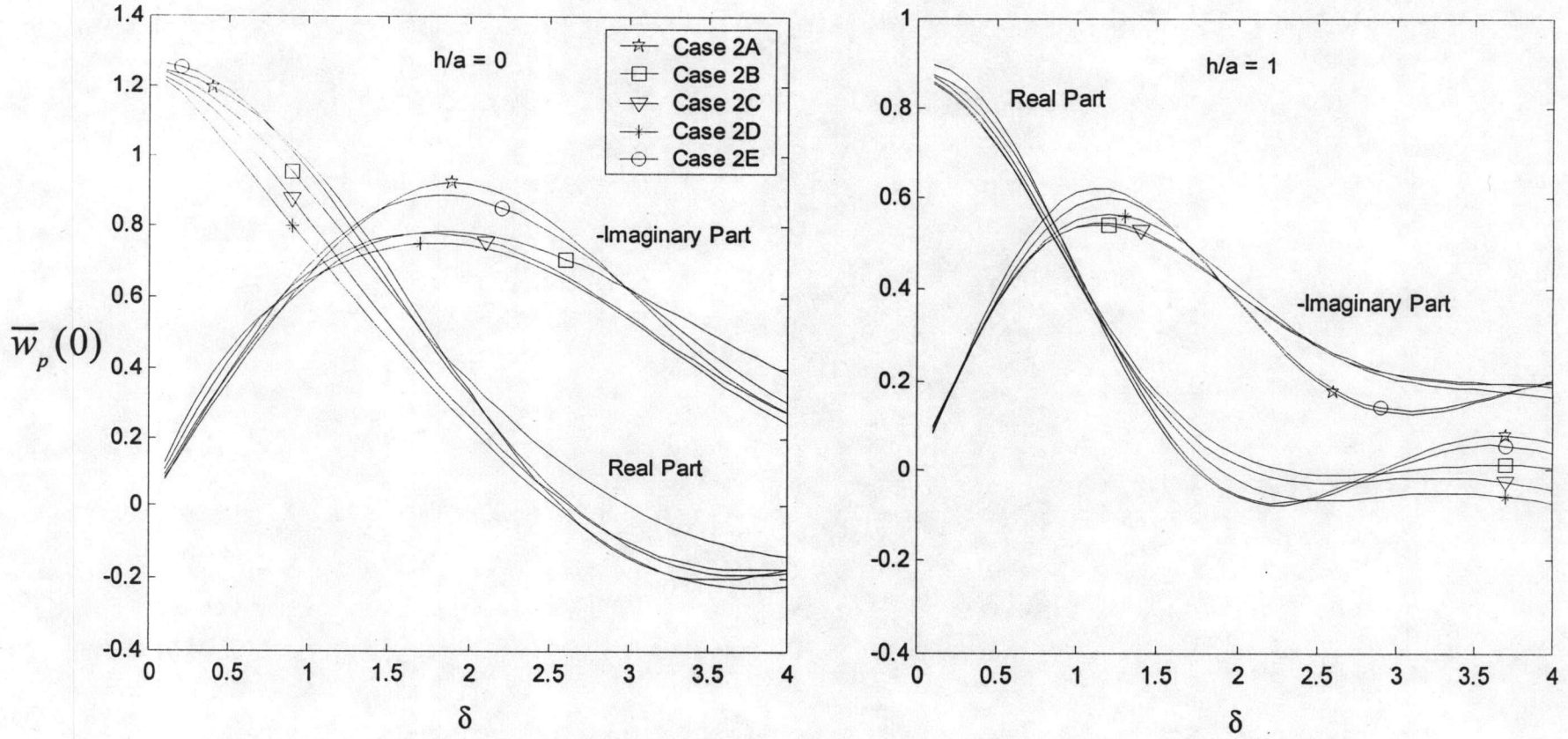


Figure 24. Central displacement of a permeable circular plate in a multi-layered poroelastic half-space

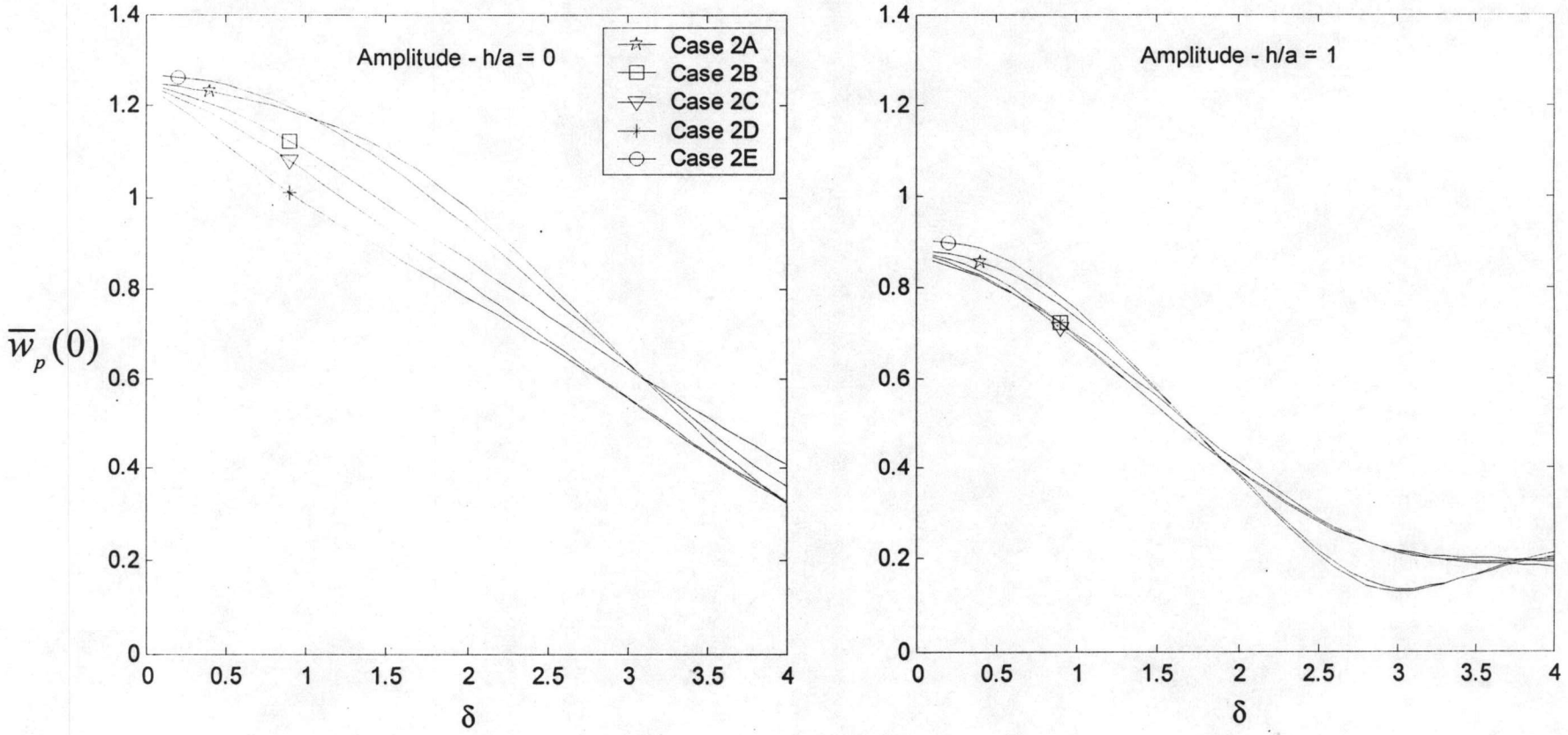


Figure 25. Amplitude of central displacement of a permeable circular plate in a multi-layered poroelastic half-space

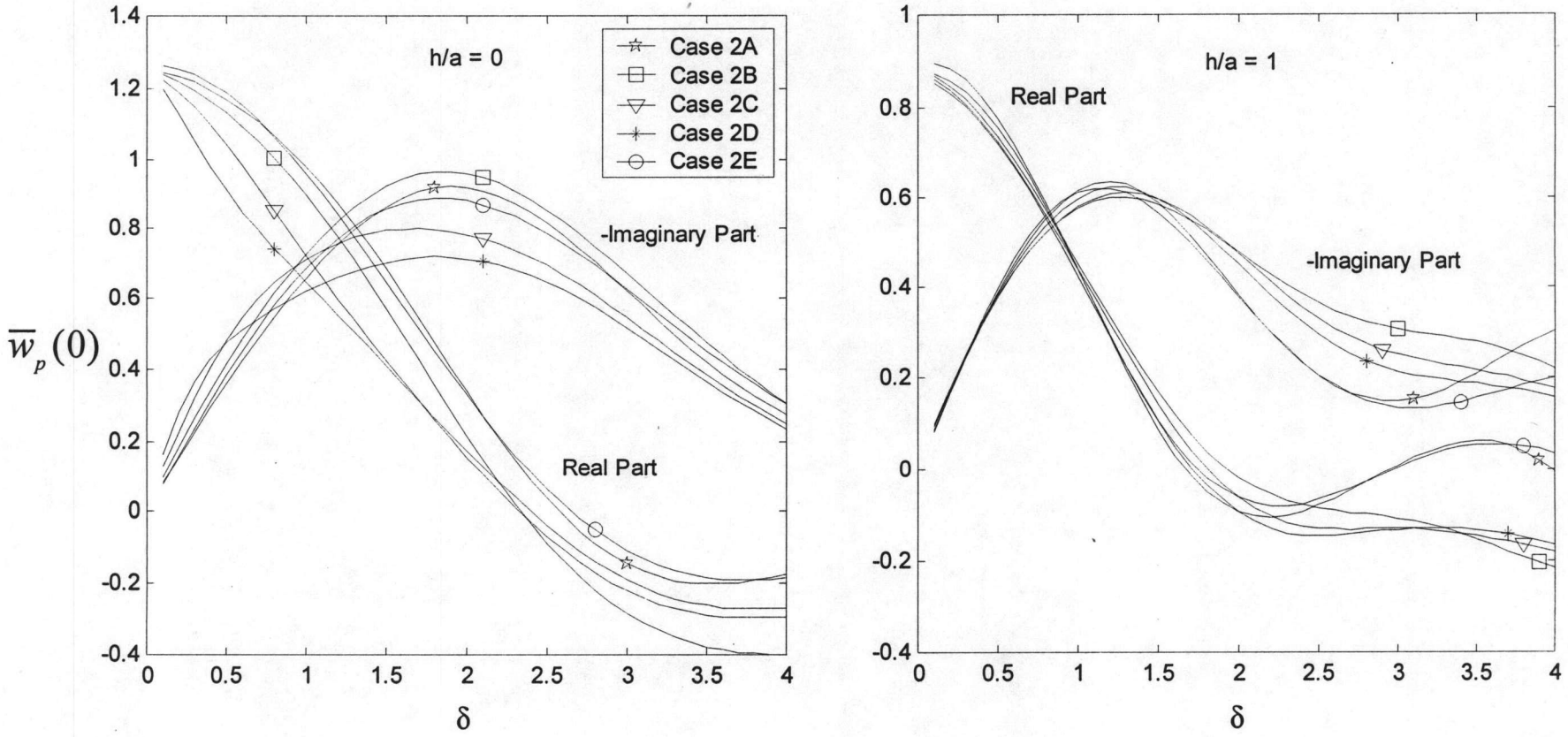


Figure 26. Central displacement of an impermeable circular plate in a multi-layered poroelastic half-space

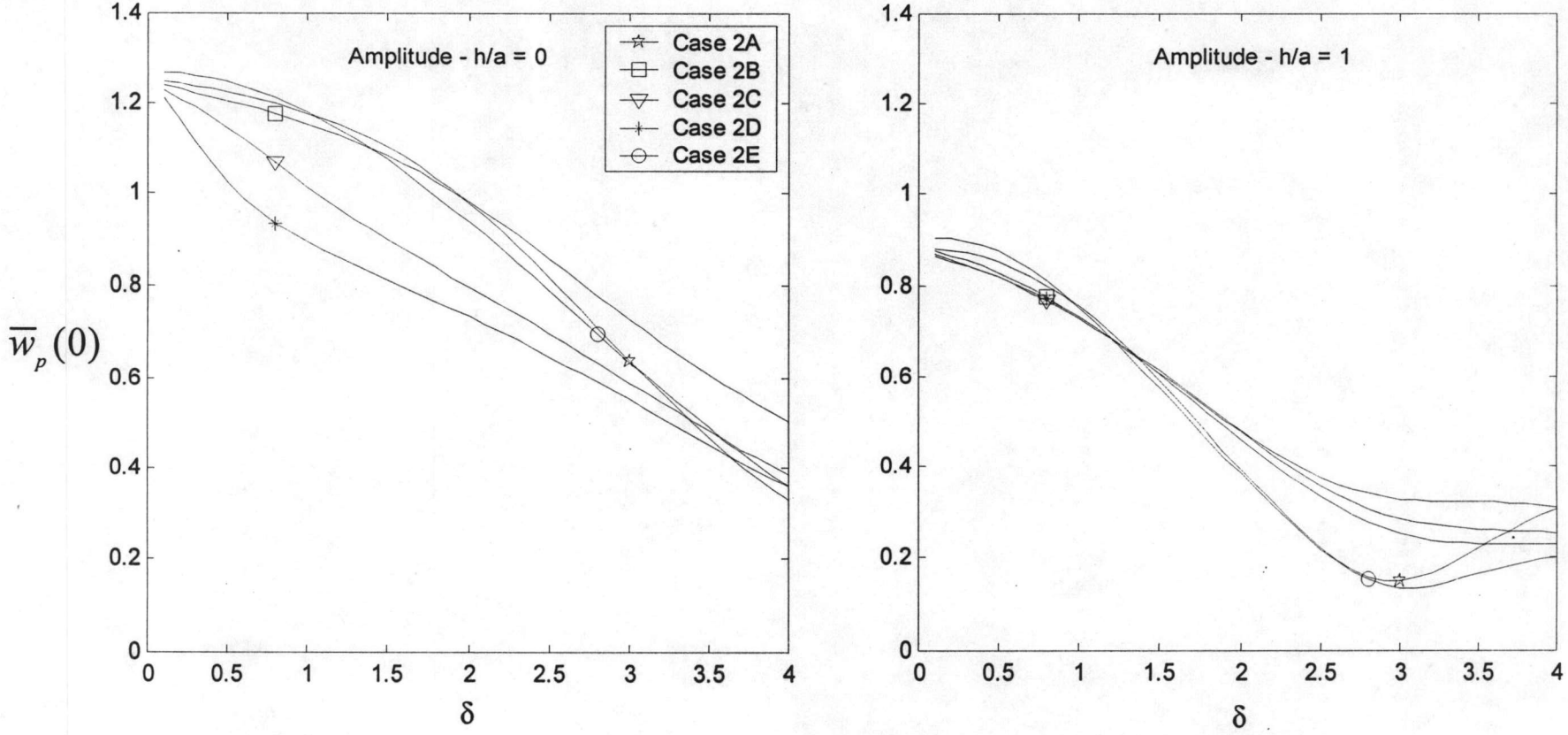


Figure 27. Amplitude of central displacement of a impermeable circular plate in a multi-layered poroelastic half-space

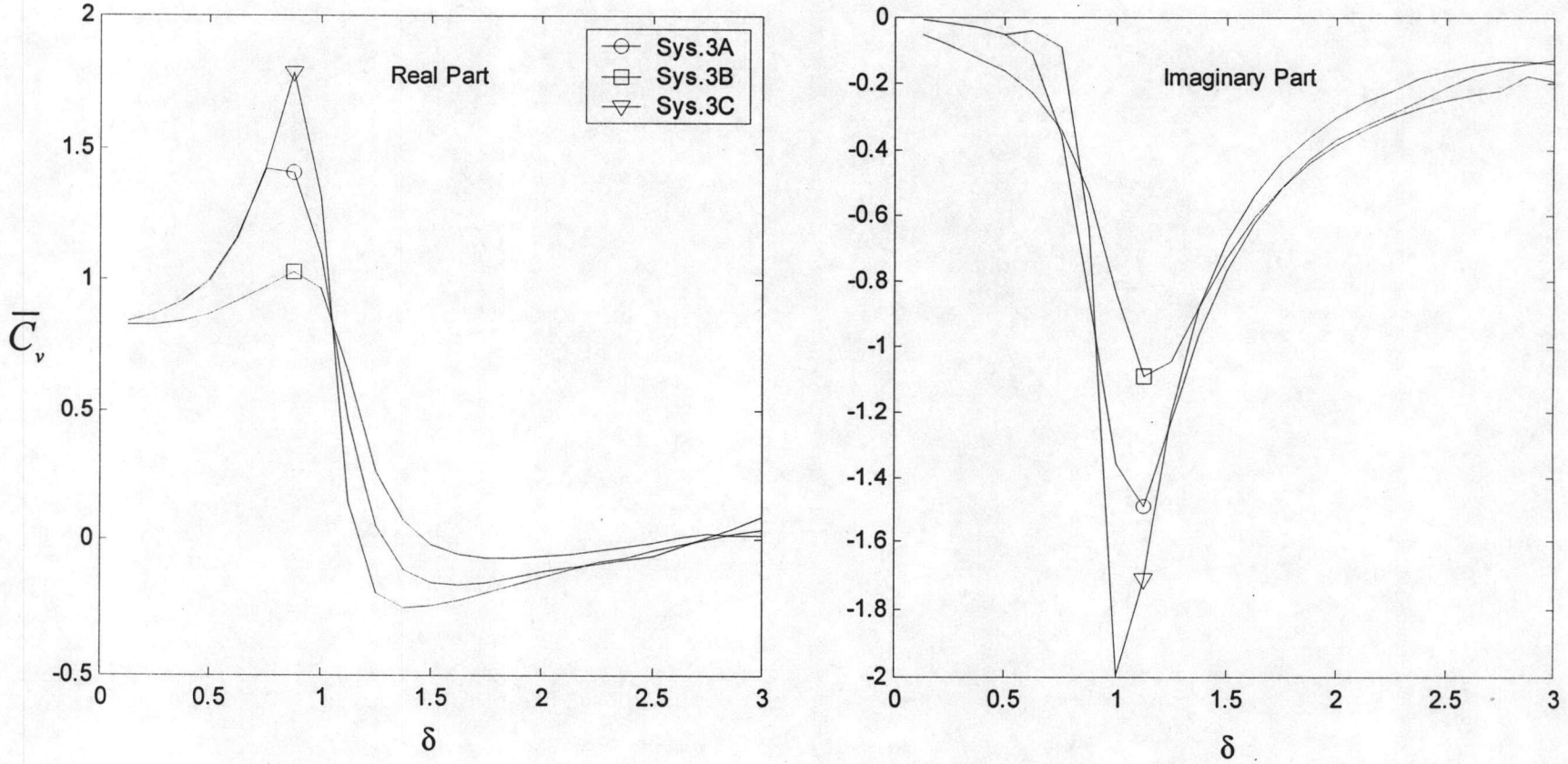


Figure 28. Vertical compliance of an impermeable rigid circular plate in a multi-layered poroelastic half-space ($h/a=1$)

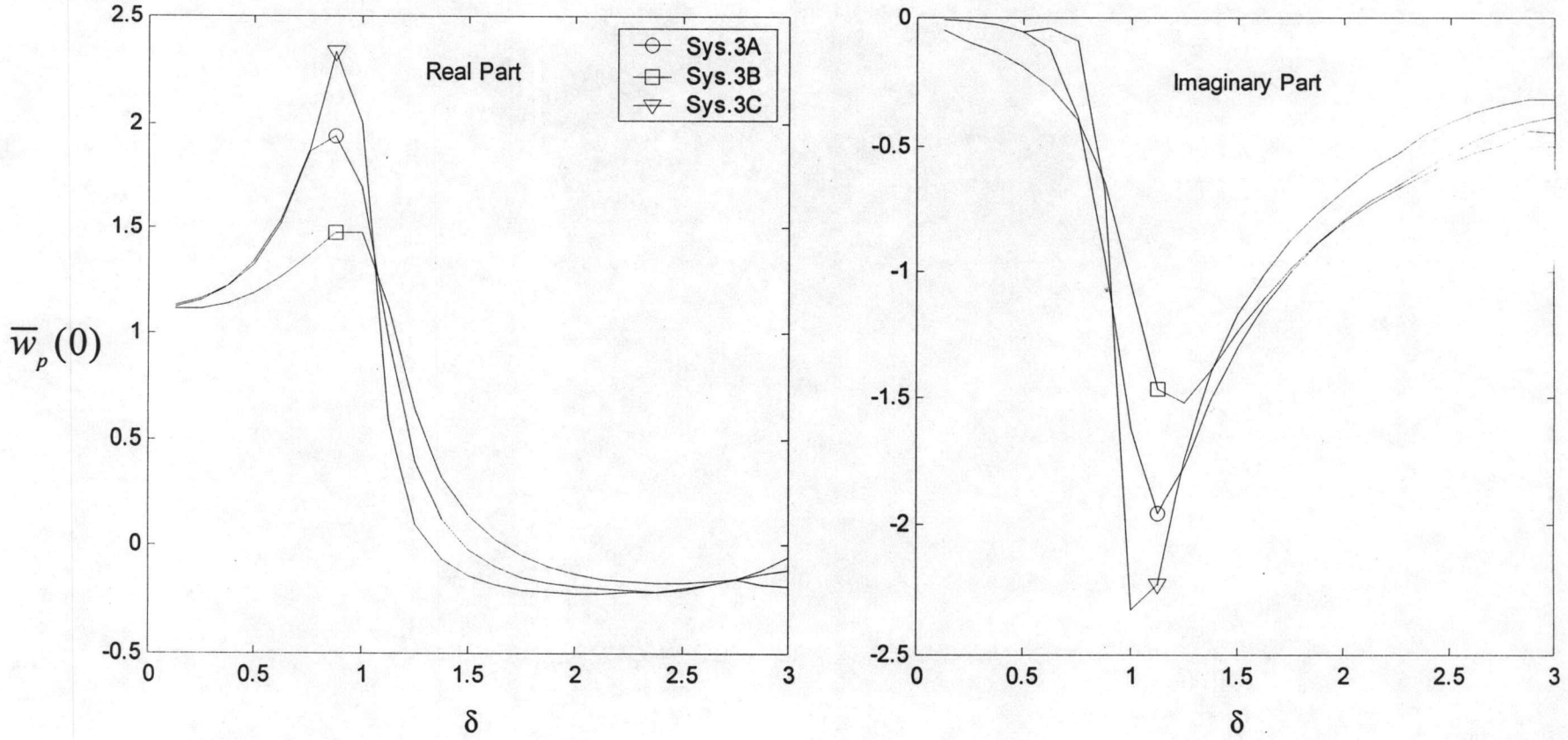


Figure 29. Central displacement of an impermeable circular plate in a multi-layered poroelastic half-space ($h/a=1$)

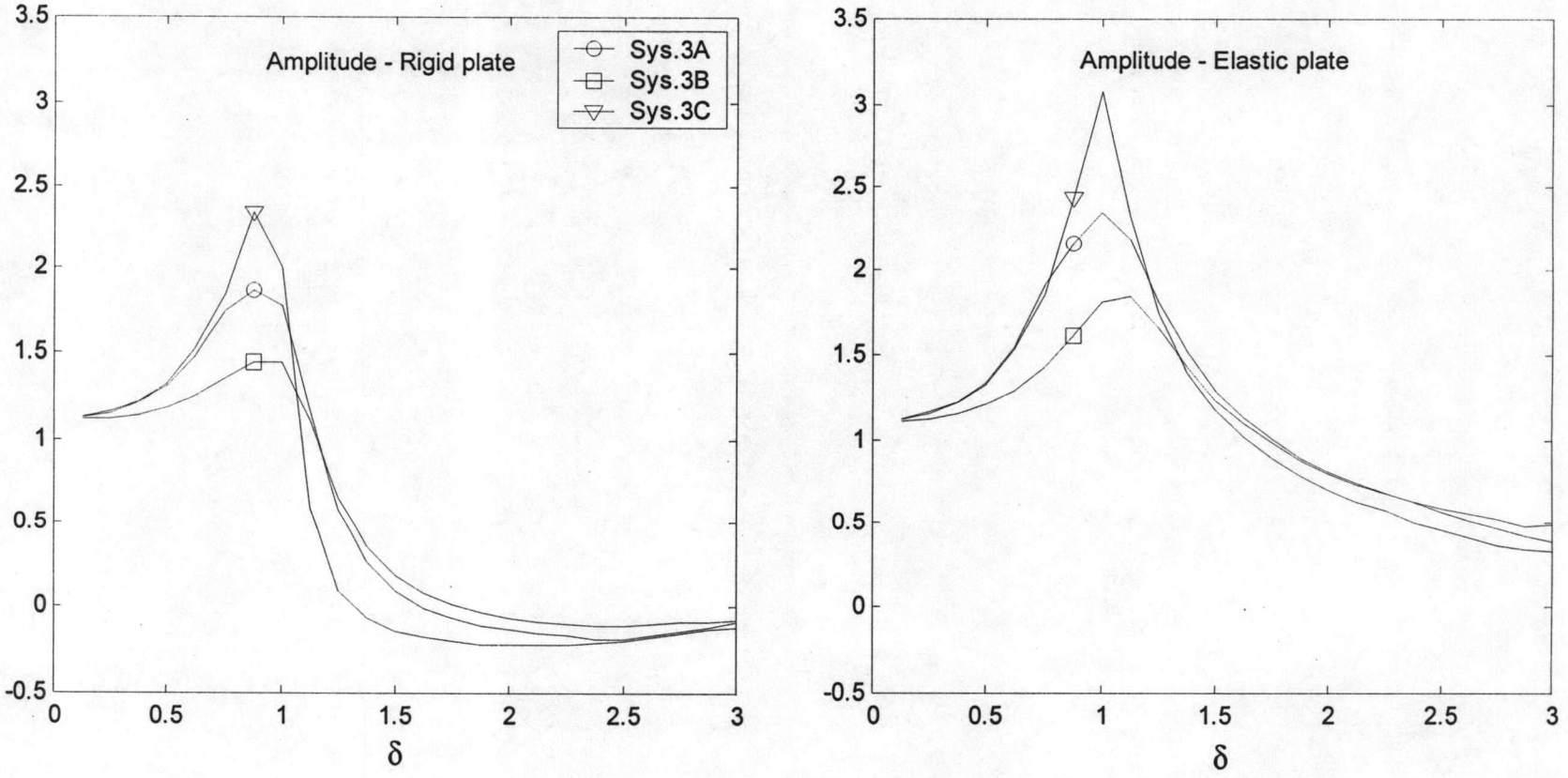


Figure 30. Amplitude of $\overline{C}_v$ and $\overline{w}_p(0)$ of an impermeable circular plate in a multi-layered poroelastic half-space ($h/a=1$)

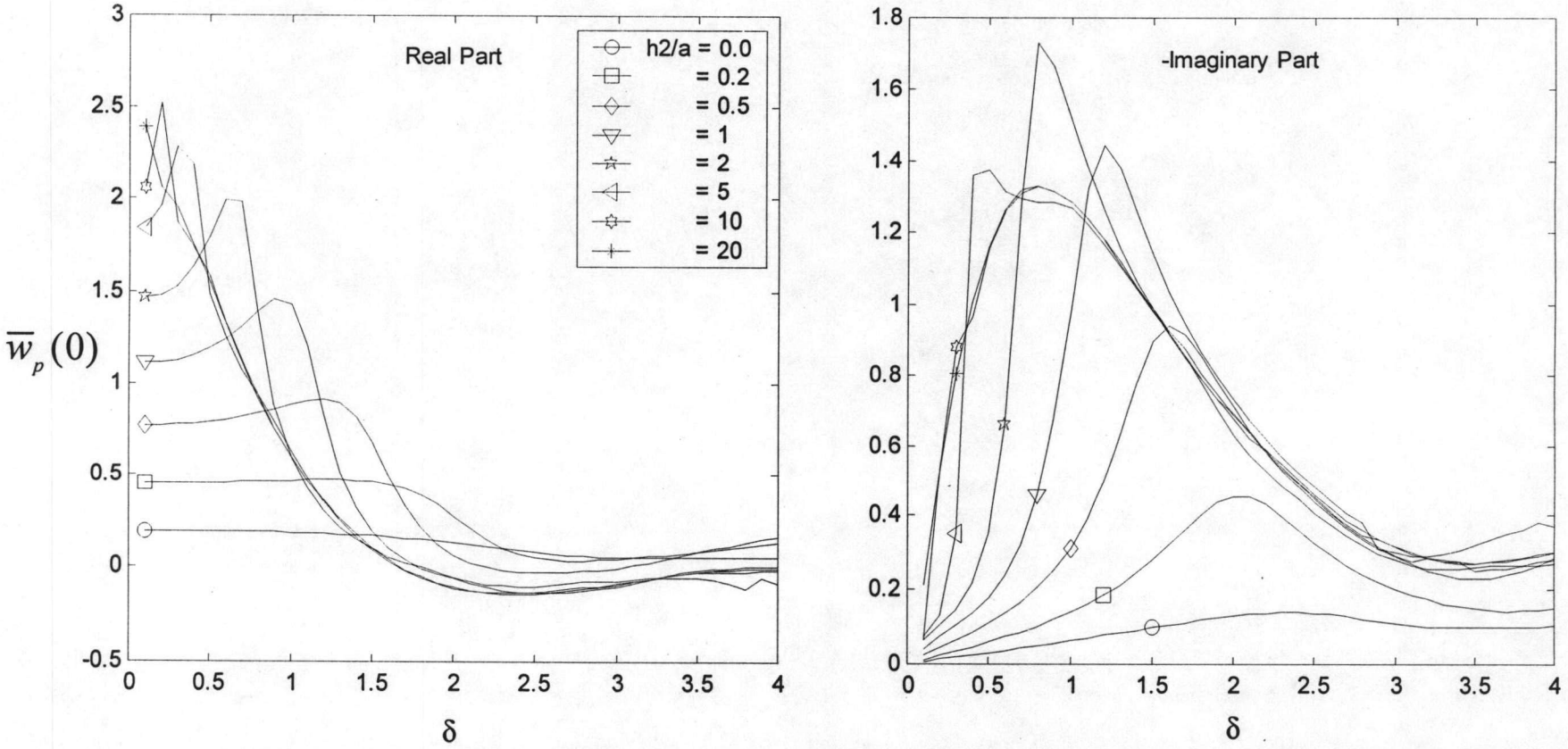


Figure 31. Central displacement of a permeable circular plate in a multi-layered poroelastic half- space with different layer thicknesses

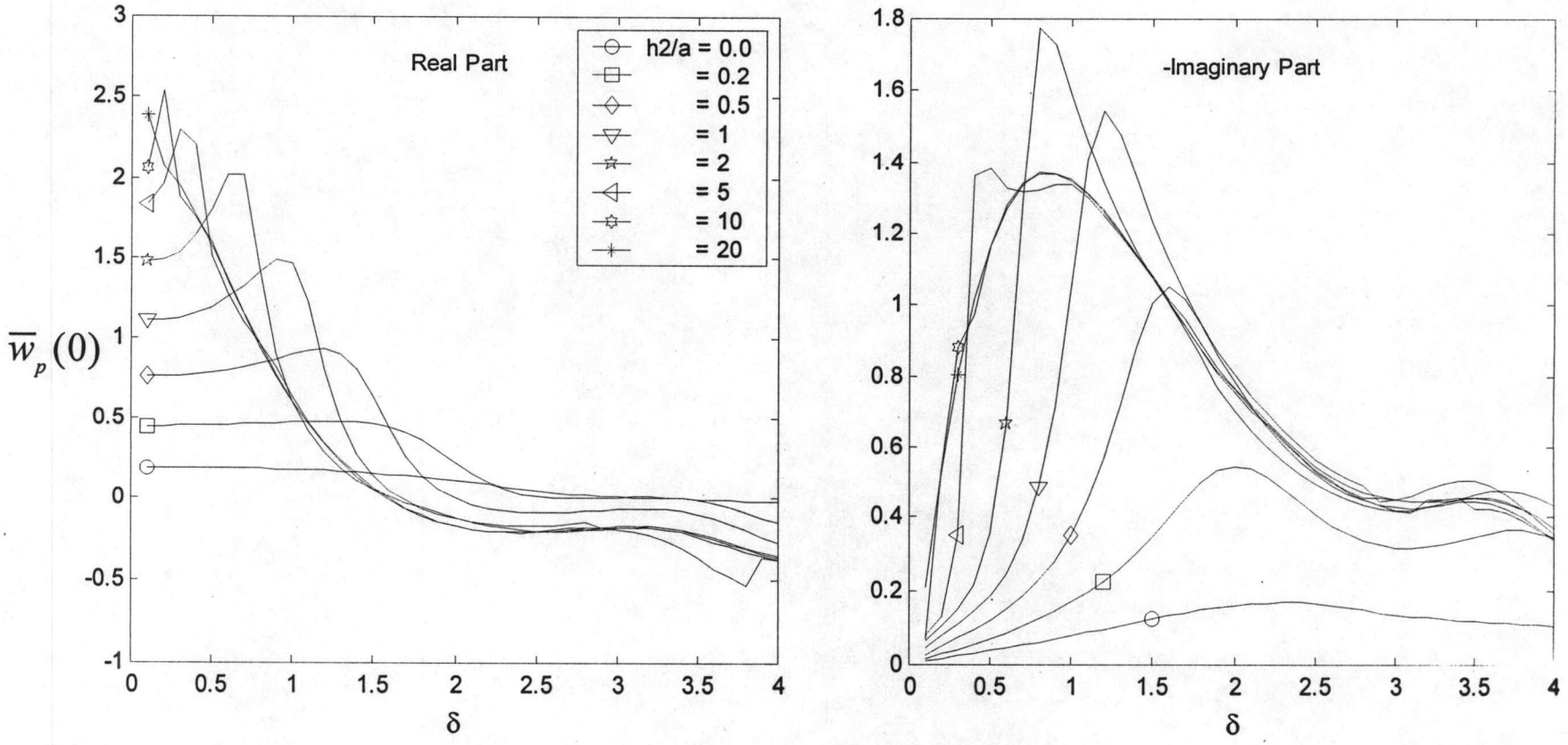


Figure 32. Central displacement of an impermeable circular plate in a multi-layered poroelastic half-space with different layer thicknesses

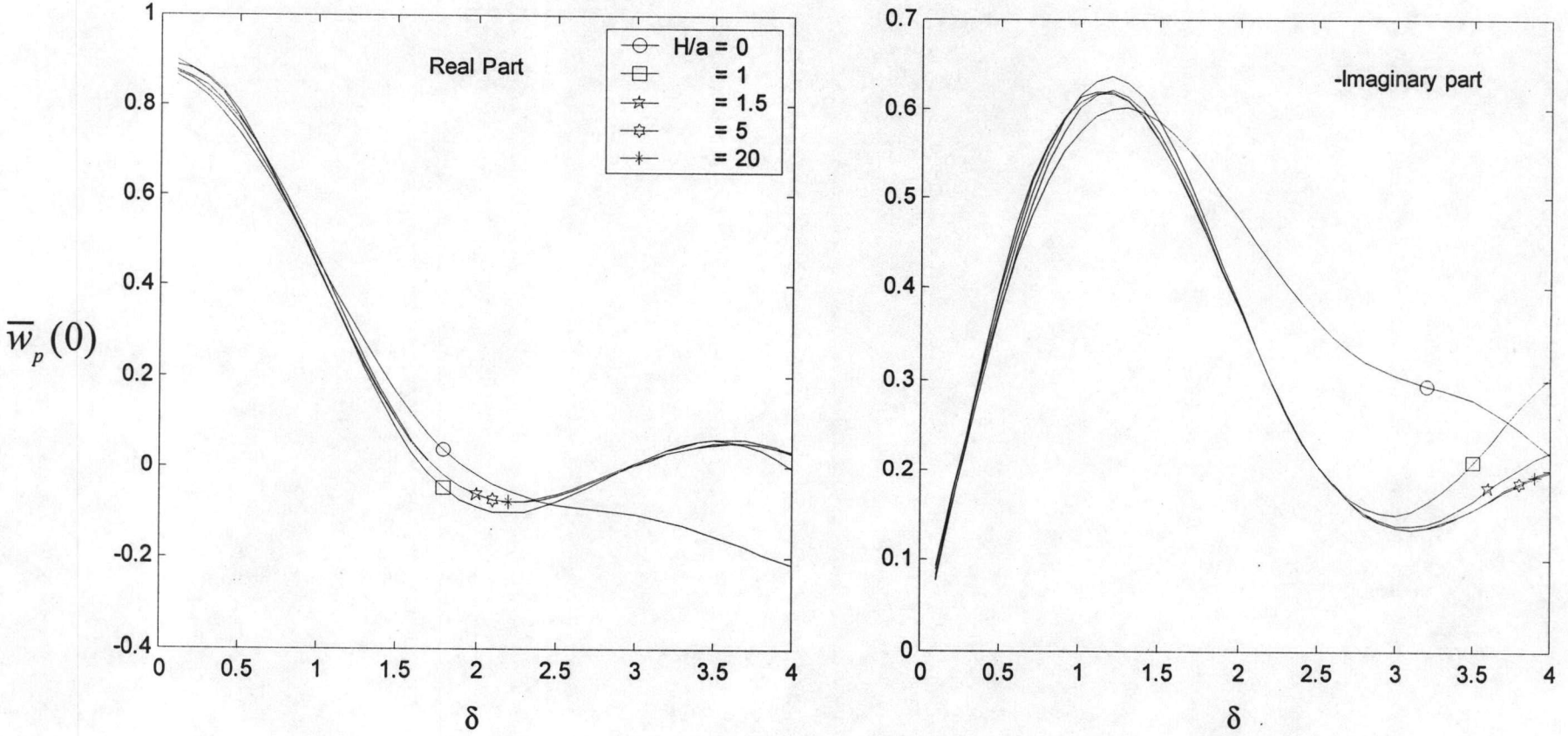


Figure 33. Central displacement of an impermeable plate in a half-space with different depths of saturation ($\hat{h}/a = 1$)

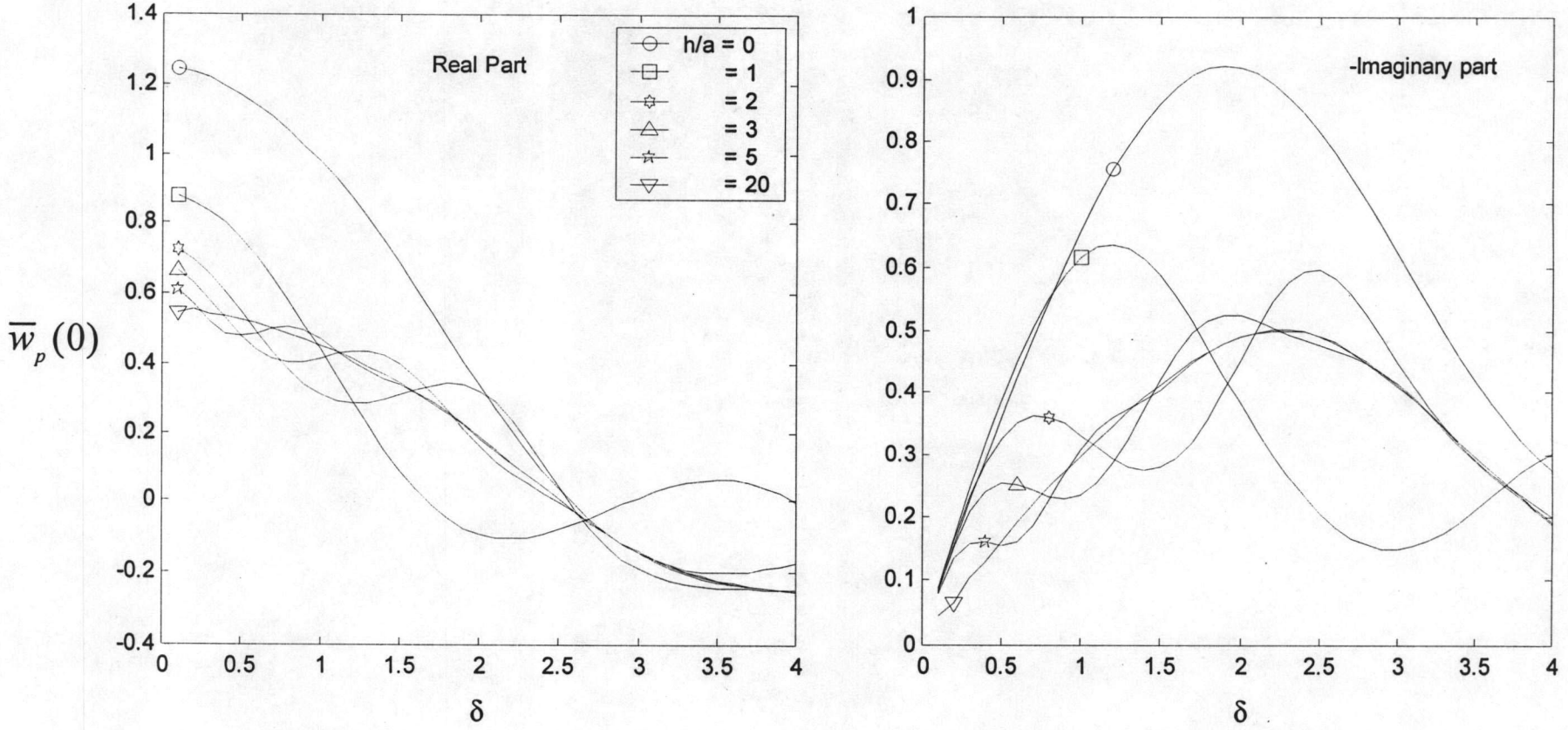


Figure 34. Central displacement of an impermeable plate in a half-space with different depths of embedment

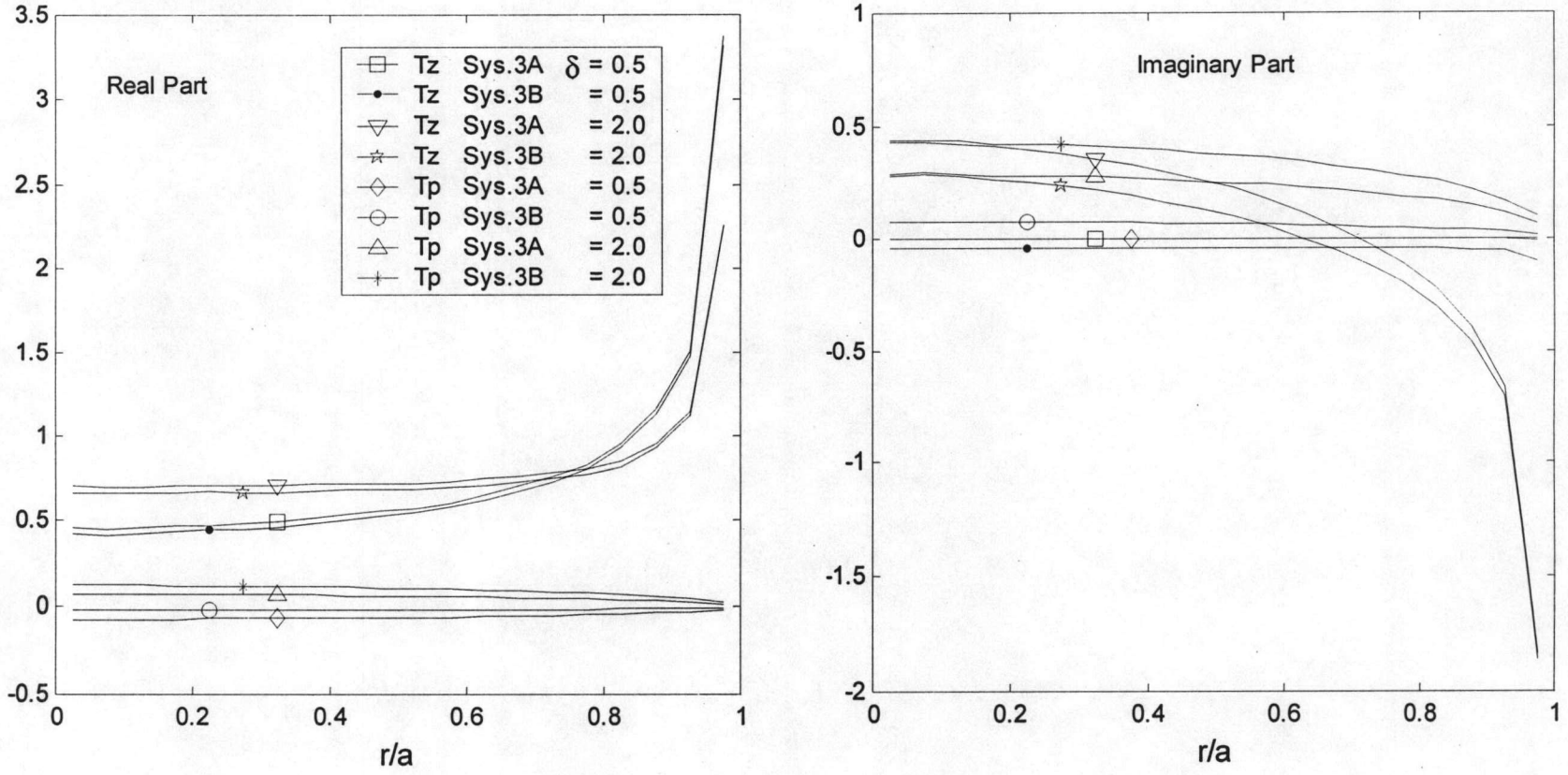


Figure 35. Profiles of vertical stress and pore pressure jumps under an impermeable rigid plate on a multi-layered poroelastic half-space